Modern Physics Letters B
© World Scientific Publishing Company

arXiv:1408.0089v2 [cond-mat.str-el] 7 Sep 2014

LATTICE GAUGE THEORY FOR CONDENSED MATTER PHYSICS: FERROMAGNETIC SUPERCONDUCTIVITY AS ITS EXAMPLE

IKUO ICHINOSE

Department of Applied Physics, Nagoya Institute of Technology, Nagoya, 466-8555, Japan

TETSUO MATSUI

Department of Physics, Kinki University, Higashi-Osaka, 577-8502, Japan

Received (Day Month Year)
Revised (Day Month Year)

Recent theoretical studies of various strongly-correlated systems in condensed matter physics reveal that the lattice gauge theory(LGT) developed in high-energy physics is quite a useful tool to understand physics of these systems. Knowledges of LGT are to become a necessary item even for condensed matter physicists. In the first part of this paper, we present a concise review of LGT for the reader who wants to understand its basics for the first time. For illustration, we choose the abelian Higgs model, a typical and quite useful LGT, which is the lattice verison of the Ginzburg-Landau model interacting with a U(1) gauge field (vector potential). In the second part, we present an account of the recent progress in the study of ferromagnetic superconductivity (SC) as an example of application of LGT to topics in condensed matter physics, . As the ferromagnetism (FM) and SC are competing orders with each other, large fluctuations are expected to take place and therefore nonperturbative methods are required for theoretical investigation. After we introduce a LGT describing the FMSC, we study its phase diagram and topological excitations (vortices of Cooper pairs) by Monte-Carlo simulations.

Keywords: Lattice gauge theory; Strongly-correlated systems; Ginzburg-Landau theory; Ferromagnetic superconductivity; Monte-Carlo simulation; Path-integral

1. Introduction

A strongly-correlated system is a set of either fermions or bosons which interact strongly each other. Such a system may exhibit collective behaviors that cannot be expected from the behaviors of each single particle, and has been the subject of great interest in various fields of condensed matter physics. For example, the $t-J$ model, which is a typical model of electrons interacting via strong Coulomb repulsion, is taken as a standard model of high-temperature superconductors[1]. Another example is the Bose Hubbard model[3] and the related bosonic $t-J$ model[4], which are to be used to study cold bosonic atoms put on an optical lattice[5] and tuned to have

large interaction parameters. In the last two decades, theoretical approach using gauge theory and the associated concepts has proved itself a convincing way to understand essentials of their physics [6,7].

The gauge theory put on a spatial lattice (and even on the imaginary discrete time in the path-integral formalism) is known as lattice gauge theory (LGT), which is introduced by Wilson in 1974 as a model of quark confinement[8]. Since then, it has contributed to increase our knowledges not only of quantum chromodynamics (QCD) itself, but also of nonperturbative aspects of general quantum field theory[9]. The reason to consider a lattice instead of the usual continuum space is to reduce the degrees of freedom from uncountable infinity to countable infinity, which allows us a concrete definition of the field theory in the nonperturbative region and also ways to examine it such as the strong-coupling (high-temperature) expansion. Concerning to the global phase structure, LGT shows, in addition to the ordinary Coulomb phase and Higgs phase of gauge dynamics (they are sometimes called deconfinement phases), the existence of so called confinement phase. This phase was crucial to explain confinement of quarks[8], one of the longstanding problem in high-energy physics, because, in the confinement phase, the potential energy $V(r)$ between a pair of static quark and anti-quark separated by the distance r increases linearly in r and costs infinite energy to separate them ($r \to \infty$). These three phases are classified by the magnitude of fluctuations of gauge field (See Table I below). The gauge field put on the lattice can be treated as periodic variables (one calls this case a compact gauge field; see Sect.2.1), and the gauge-field configurations reflecting this periodicity may involve large spatial variations beyond the conventional perturbative ones. Monopoles are a typical and important example of such configurations (monopoles in the continuum gauge theory cost infinite energy and so not possible). In the confinement phase, such monopoles condense[10], and the resulting strong fluctuations of gauge field are argued to generate squeezed one-dimensional line of electric flux (variables conjugate the the gauge field itself). Then, in the confinement phase, such an electric flux gives rise to the linearly-rising confining potential. This phenomenon of formation of electric fluxes is sometimes called the "dual" Meissner effect in contrast to the Meissner effect in ordinary superconductors where magnetic field is squeezed into magnetic fluxes due to Cooper-pair condensation. One way to recognize the relevance of monopoles among other possible (topological) excitations is to perform the duality transformation[11], which rewrites the system as an ensemble of monopoles or monopole loops.

hase	fluctuation of gauge field	potential energy $V(r)$
Higgs	small	$\propto \frac{\exp(-mr)}{r}$
Coulomb	medium	$\propto \frac{1}{r}$
Confinement	large	$\propto r$

Table 1. Three phases of gauge dynamics: $V(r)$ is the potential energy stored between a pair of point charges with the opposite signs and separated by the distance r.

Also, in some restricted fields of condensed matter physics, LGT has been applied successfully. One example is the $t-J$ model of high-T_c superconductivity (SC)[6]. Here the strong correlations are implemented by excluding the double occupancy state of electrons, the state of two electrons with the opposite spin directions occupying the same site, from the physical states. This may be achieved by viewing an electron as a composite of fictitious particles, a so-called holon carrying the charge degree of freedom of the electron and a spinon carrying the spin degree of freedom[12]. By the method of auxiliary field in path-integral, one may introduce U(1) gauge field which binds holon and spinon. Then the possible phases may be classified according to the dynamics of this U(1) gauge field. In the confinement phase, the relevant quasiparticles are the original electrons in which holons and spinons are confined. This corresponds to the state at the overdoped high temperature region. In the deconfinement Coulomb phase, quasiparticles are holons and spinons in which charge and spin degrees of freedom behave independently. This phenomenon is called the charge-spin separation[13] and are to describe the anomalous behavior of the normal state such as the liner-T resistivity. Further correspondence between the gauge dynamics and the observed phases are also satisfactory as discussed in Refs.[1,6,13]. In particular, possibility of experimental observation of spinons is discussed in Ref.[2].

Another application of LGT to relate the dynamics of auxiliary gauge field and the observed phases is the (fractional) Hall effect[14]. Among a couple of parallel formulations[15], one may view an electron as a composite of a so called bosonic fluxon carrying fictitious (Chern-Simons) gauge flux and a so called fermionic chargon carrying the electric charge[7]. In the deconfinement phase, these fluxons and chargons are separated, i.e., particle-flux separation takes place. If fluxons Bose condense at sufficiently low temperatures, the resulting system is fermionic chargons in a reduced uniform magnetic field. These chargons are nothing but the Jain's composite fermions, and the integer Hall effect of them explain the fractional Hall effect of the original electron system.

In this paper, we shall see yet another example of LGT approach to condensed matter physics. Namely, we consider a lattice model of ferromagnetic SC, which exhibits the ferromagnetism (FM) and/or SC, two typical and important phenomena in condensed matter physics. We note here that the introduction of a spatial lattice in the original LGT in high-energy theory is traced back, as mentioned, to the necessity to define a nonperturbative field theory. The lattice spacing there should be taken as a running cutoff(scale) parameter in the renormalization-group theory[18] and the continuum limit should be taken carefully. However, in condensed matter physics, introduction of a lattice has often a practical support independent of the above meaning, i.e., the system itself has a lattice structure. One may naturally regard the lattice of the model as the real lattice of material in question. In this paper, we shall not touch the continuum limit in the sense of renormalization group.

The layout of the paper is as follows: In Sect. 2, we review LGT. The reader who is not familiar with this subject may acquire necessary knowledge to understand

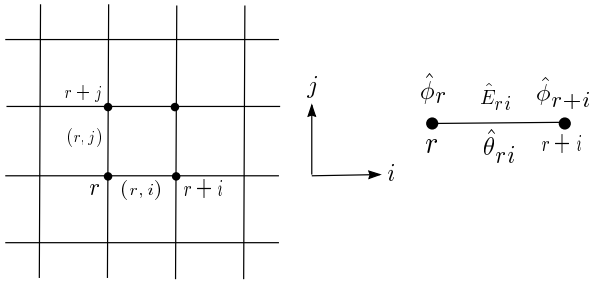

Fig. 1. $i-j$ plane of the 3d lattice and $\hat{\phi}_r$ defined on the site r and $\hat{\theta}_{ri}$ and $\hat{E}_{ri}$ defined on the link $(ri) = (r, r+i)$.

the successive sections. In Sect. 3, we explain the lattice model of ferromagnetic superconductivity (FMSC). It is based on the known Ginzburg-Landau theory defined in the continuum space. In Sect. 4, we present numerical results of Monte Carlo simulations for the lattice model in Sect. 3. In Sect. 5, we give conclusion.

2. Introduction to lattice gauge thoery

Formulating field-theoretical models by using space(-time) lattice is quite useful for studying their properties nonperturbatively. In particular, because of the lattice formulation itself, the high-temperature expansion (strong-coupling expansion) can be performed analytically even for the case in which fluctuations of the fields are very strong. Furthermore, numerical studies like the Monte-Carlo simulation can be applicable for wide range of the lattice field theories. In this section, we review LGT consisting of a U(1) gauge field and a charged bosonic matter field.

2.1. *Lattice gauge theory in Hamiltonian formalism*

In this subsection, we explain the Hamiltonian formalism of LGT[16]. The reasons are two fold: (i) it gives rise to an intuitive picture of the relevant states in terms of electric field and magnetic field, and (ii) it plays an important role in recent development in quantum simulations of the dynamical gauge field by using ultracold atomic systems put on an optical lattice.

Let us start with an example of Hamiltonian system defined on a three-dimensional ($d = 3$) spatial cubic lattice with lattice spacing a. Its sites are labeled by r, and its links (bonds) are labeled as (r, i) where i is the direction index $i = 1, 2, 3$. We sometimes use i also for the unit vector in the ith-direction, such as $(r, i) = (r, r + i)$ (See Fig.1).

One may put matter fields on each site r, which may be bosons/fermions composing materials in question, e.g., electrons, atoms in an optical lattice, Coope-pair field of SC, spins, or even more complicated ones. For definiteness, we put below a one-component canonical nonrelativistic boson field[17], whose annihilation and

creation operators $\hat{\phi}_r, \hat{\phi}_r^\dagger$ satisfy

$$[\hat{\phi}_r, \hat{\phi}_{r'}^\dagger] = \delta_{rr'}. \tag{2.1}$$

Gauge fields are put on each link (r, i) in LGT (See Fig.1). They may be associated with the gauge group U(1), SU(N), etc, and meditate interactions between matters. They are viewed as connections in differential geometry that relate two local frames of the internal space of matter field at neighboring lattice sites r and $r + i$. For definiteness, we consider below a U(1) gauge field operator $\hat{\theta}_{ri}$ $(= \hat{\theta}_{ri}^\dagger)$. This is viewed as the lattice version of well-known vector potential field $\hat{A}_i(r)$ (we use the same letter r for the coordinate of the continuum space) describing the electromagnetic(EM) interaction, but may have different origins, e.g., mediating interactions between holons and spinons, as explained in Section 1. The momentum operator $\hat{E}_{ri}$ conjugate to $\hat{\theta}_{ri}$ describes the electric field and satisfy

$$[\hat{\theta}_{ri}, \hat{E}_{r'j}] = i\delta_{rr'}\delta_{ij},\ [\hat{\theta}_{ri}, \hat{\theta}_{r'j}] = [\hat{E}_{ri}, \hat{E}_{r'j}] = 0. \tag{2.2}$$

To understand the LGT Hamiltonian, it is helpful to start with a model Hamiltonian $\hat{H}_{\rm c}$ defined in the continuum space. Let us consider the following Ginzburg-Landau(GL)-type model:

$$H_{\rm c} = \int d^3r \Big[\sum_i |D_i\hat{\phi}(r)|^2 + m^2\hat{\rho}(r) + \lambda\hat{\rho}(r)^2 + \frac{1}{2}\sum_i \hat{E}_i(r)^2 + \frac{1}{4}\sum_{i,j} \hat{F}_{ij}(r)^2 \Big],$$
$$D_i = \partial_i + ig\hat{A}_i(r),\ \hat{\rho}(r) = \hat{\phi}^\dagger(r)\hat{\phi}(r),\ \hat{F}_{ij}(r) = \partial_i\hat{A}_j(r) - \partial_j\hat{A}_i(r), \tag{2.3}$$

where D_i is the covariant derivative expressing the minimal coupling of ϕ-particle with the EM field, g is the coupling constant (charge of ϕ-particle[20]), m, λ are GL parameters whose meaning is explained later, and $\hat{F}_{ij}(r)$ is the magnetic field $B_i(r) = \epsilon_{ijk}F_{jk}(r)$. One may check that the each term of $H_{\rm c}$ is invariant under the local gauge transformation,

$$\hat{\phi}(r) \to e^{i\Lambda(r)}\hat{\phi}(r),\ \hat{A}_i(r) \to \hat{A}_i(r) - \frac{1}{g}\partial_i\Lambda(r),\ \hat{E}_i(r) \to \hat{E}_i(r), \tag{2.4}$$

for an arbitrary function $\Lambda(r)$. By using the canonical commutation relations $[\hat{\phi}(r), \hat{\phi}^\dagger(r')] = \delta^{(3)}(r - r')$ and $[\hat{A}_i(r), \hat{E}_j(r')] = i\delta_{ij}\delta^{(3)}(r - r')$, one may check that its generator $\hat{Q}(r)$ is given by

$$\hat{Q}(r) = \sum_i \partial_i\hat{E}_i(r) - g\hat{\rho}(r), \tag{2.5}$$

and $\hat{Q}(r)$ commutes with $\hat{H}_{\rm c}$, $[\hat{Q}(r), \hat{H}_{\rm c}] = 0$. So one may define the physical states $|{\rm phys}\rangle$ so that they are eigenstates of $\hat{Q}(r)$ (superselection rule). In the usual case, i.e., when there are no external electric field, one imposes the local constraint,

$$\hat{Q}(r)|{\rm phys}\rangle = 0, \tag{2.6}$$

which leads to the lattice version of the Gauss' law $\hat{Q}_r = 0$ [See Eq.(2.17].

Now we consider the Hamiltonian on the cubic lattice. In LGT, the operator $\hat{\theta}_{ri}$ defined on link (r, i) is assumed to approach as $\hat{\theta}_{ri} \to ag\hat{A}_i(r)$ as the lattice

spacing a becomes small. Furthermore, as we shall see, the natural U(1) gauge field operator in LGT is not $\hat{\theta}_{ri}$ but its exponential,

$$\hat{U}_{ri} \equiv \exp(i\hat{\theta}_{ri}),\ \hat{U}_{ri}^{\dagger}\hat{U}_{ri} = \hat{1}, \tag{2.7}$$

and so $\hat{\theta}_{ri}$ is viewed as an angle operator (we discuss this point in detail later). Then, by using Eq.(2.2) we have $\hat{E}_{ri} \to a^2 E_i(r)$ as $a \to 0$ (note $\hat{E}_{ri}$ is dimensionless and $\delta^{(3)}(r) \simeq \delta_{r0}a^{-3}$) and

$$[\hat{E}_{ri}, \hat{U}_{r'j}] = \delta_{ij}\delta_{rr'}\hat{U}_{ri}. \tag{2.8}$$

(Note that Eq.(2.2) implies the replacement $\hat{E}_{ri} \to -i\partial/\partial\theta_{ri}$.) To construct a set of eigenstates satisfying the completeness conditions, let us start with a pair of operators $\hat{U}$ and $\hat{E}$ sitting on certain link (we suppress their link index). Then we have

$$\begin{aligned}
&\hat{U}|\theta\rangle = e^{i\theta}|\theta\rangle,\ \theta \in [0, 2\pi\},\ \hat{E}|n\rangle = n|n\rangle,\ n \in \mathbf{Z},\\
&\langle\theta|n\rangle = \frac{e^{in\theta}}{\sqrt{2\pi}},\ \hat{1}_U = \int_0^{2\pi} d\theta|\theta\rangle\langle\theta|,\ \hat{1}_E = \sum_{n=-\infty}^{\infty}|n\rangle\langle n|.
\end{aligned} \tag{2.9}$$

So $\hat{\theta}$ and $\hat{E}$ correspond to the position and momentum operators in the ordinary quantum mechanics respectively, but the significant difference is that the theory is taken to be *compact*, i.e., the physical state $|\mathrm{phys}\rangle$ is imposed to be periodic in θ,

$$\langle\theta|\mathrm{phys}\rangle = \langle\theta + 2\pi|\mathrm{phys}\rangle, \tag{2.10}$$

which implies that the eigenvalues are an angle $\theta \in [0, 2\pi)$ defined by mod 2π, and integers n, instead of two real numbers. Because one may write

$$|n\rangle = \hat{1}_U|n\rangle = \int \frac{d\theta}{\sqrt{2\pi}} e^{in\theta}|\theta\rangle = e^{in\hat{\theta}} \cdot \int \frac{d\theta}{\sqrt{2\pi}}|\theta\rangle = e^{in\hat{\theta}}|n=0\rangle = \hat{U}^n|n=0\rangle, \tag{2.11}$$

$\hat{U}^{(\dagger)}$ is just the creation (annihilation) operator of the electric field of unit electric flux (the signature of n distinguishes the direction of the flux), which is called a "string bit". These relations remind us the analogy with the angular momentum operators $\vec{L}$ as $\hat{E} \leftrightarrow \hat{L}_z (n \leftrightarrow L_z/\hbar), \hat{U} \leftrightarrow \hat{L}_x + i\hat{L}_y, \theta \leftrightarrow \varphi$ (azimuthal angle) with the limit of large angular momentum $\ell \to \infty$. We note that there holds the uncertainty principle,

$$\Delta\theta \cdot \Delta n \geq \frac{1}{2}. \tag{2.12}$$

The Hamiltonian $\hat{H}$ of LGT should (i) reduce to $\hat{H}_c$ of Eq.(2.3) in the naive continuum limit $a \to 0$, and (ii) respect the U(1) local gauge symmetry as in the continuum. A simple example of $\hat{H}$ satisfying these two conditions is given by

$$\begin{aligned}
\hat{H} &= t\sum_{r,i}(\hat{\phi}_{r+i}^{\dagger} - \hat{U}_{ri}\hat{\phi}_r^{\dagger})(\hat{\phi}_{r+i} - \hat{U}_{ri}^{\dagger}\hat{\phi}_r) + \sum_r V(\hat{\phi}_r) + \hat{H}_{\mathrm{g}},\\
\hat{H}_{\mathrm{g}} &= \frac{g^2}{2a}\sum_{r,i}(\hat{E}_{ri})^2 + \frac{1}{2g^2 a}\sum_r\sum_{i<j}\Big(\hat{U}_{rj}\hat{U}_{r+j,i}\hat{U}_{r+i,j}^{\dagger}\hat{U}_{ri}^{\dagger} + \mathrm{H.c.} - 2\Big).
\end{aligned} \tag{2.13}$$

Here $V(\hat{\phi}_r)$ represents the self-interaction of $\hat{\phi}_r$. The naive continuum limit of $\hat{H}$ is checked as $\hat{H} \to \hat{H}_c + O(a^2)$ with a suitable choice of $V(\hat{\phi}_r)$ by using the following relations as $a \to 0$:

$$\hat{\phi}_r \to a^{\frac{3}{2}}\hat{\phi}(r),\ \hat{U}_{ri} \to e^{iga\hat{A}_i(r)} \simeq 1 + iga\hat{A}_i(r) - \frac{a^2g^2}{2}(\hat{A}_i(r))^2,$$
$$\hat{E}_{ri} \to \frac{a^2}{g}\hat{E}_i(r),\ \sum_r \to \frac{1}{a^3}\int d^3r. \tag{2.14}$$

In particular, the last $UUUU$-term reduces to the magnetic term FF as

$$UUUU + \text{c.c.} \to \exp[iga(A + A - A - A)] + \text{c.c.}$$
$$= \exp[iga^2(\partial_i A_j(r) - \partial_j A_i(r))] + \text{c.c.} \to 2\cos(ga^2F_{ij}(r)) \to 2 - g^2a^4F_{ij}^2(r). \tag{2.15}$$

For gauge invariance, one may define the gauge transformation on the lattice as

$$\hat{U}_{ri} \to V_{r+i}^*\hat{U}_{ri}V_r,\ V_r = e^{i\Lambda_r} \in \mathbf{U}(\mathbf{1}),\ \hat{\phi}_r \to V_r\hat{\phi}_r, \tag{2.16}$$

which reduces to Eq.(2.4) by scaling $\Lambda_r \to \Lambda(r)$ as $a \to 0$, and check that each term of $\hat{H}$ is invariant under Eq.(2.16). We define the physical states in the same manner as in the continuum case,

$$Q_r \equiv \sum_i \nabla_i\hat{E}_{ri} - \hat{\phi}_r^\dagger\hat{\phi}_r,\ [\hat{H}, \hat{Q}_r] = 0,\ \hat{Q}_r|\text{phys}\rangle = 0, \tag{2.17}$$

where the forward difference operator ∇_i is defined as $\nabla_i f_r \equiv f_{r+i} - f_r$. Both $\nabla_i\hat{E}_{ri}$ and $\hat{\phi}_r^\dagger\hat{\phi}_r$ have integer eigenvalues. We note that $\hat{H}$ of Eq.(2.13) has the periodicity $\hat{\theta}_{ri} \to \hat{\theta}_{ri} + 2\pi$, which may be regarded as a gauge symmetry under a special gauge transformation $\Lambda_r = 2\pi r_i$.

2.2. *Physical properties of LGT*

Let us discuss the expected properties of the model (2.13). First, we focus on the case of pure gauge theory $\hat{H}_{\rm g}$ without matter field. In te continuum theory, the corresponding system,

$$\hat{H}_{\rm g} \to \frac{1}{2}\int d^3r \sum_i \Big(\hat{E}_i(r)\hat{E}_i(r) + \hat{B}_i(r)\hat{B}_i(r)\Big), \tag{2.18}$$

is well known to describe the ensemble of free photons. In contrast, $\hat{H}_{\rm g}$ on the lattice is an *interacting* theory. One can confirm it from $\cos(ga^2F_{ij}(r))$ in Eq.(2.15). It contains, in addition to the leading $F_{ij}(r)^2$ term, $F_{ij}(r)^4$ and higher interaction terms describing scattering of gauge bosons. These terms are traced back to the compactness of the model (the periodicity (2.10)).

For large $g \gg 1$, which is called the strong coupling region, one may take the electric term as the unperturbed Hamiltonian and the magnetic term as a perturbation. By recalling Eq.(2.17), the unperturbed eigenstate $|\text{eigen}\rangle$ is the eigenstate of $\hat{E}_{ri}$ with their eigenvalues satisfying the divergenceless condition. A simple example

is an electric flux of strength n along a closed loop C on the 3D lattice. The general eigenstate may be composed of such loops. So one may write

$$|\text{eigen}\rangle = \prod_k \prod_{\ell_k \in C_k} (\hat{U}_{\ell_k})^{n_k} |0\rangle, \tag{2.19}$$

where C_k denotes the k-th flux loop, ℓ_k denotes links composing C_k, and n_k is the strength of the k-th flux. If there are two external sources of charge g at r_1 and $-g$ at r_2, the lowest-energy state is an electrix flux state forming a straight line $\tilde{C}_{12}$ (on the lattice) connecting these two charges and written as

$$\prod_{\ell \in \tilde{C}_{12}} \hat{U}_\ell |0\rangle, \tag{2.20}$$

(See Fig.2a). This state has an energy $g^2/(2a)\times$ number of links in C_{12}, thus proportional to the distance r. If these two charges are quark and antiquark, isolation of each quark from the other implies $r \to \infty$ and costs infinite amount of energy, being impossible to be realized. This is Wilson's explanation of quark confinement[8].

On the other hand, for the weak-coupling region, $g \ll 1$, the magnetic term is leading. Up to the gauge transformation, the energy eigenstates in the limit $g \to 0$ should be the eigenstate of $\hat{\theta}_{ri}$ in contrast to the strong-coupling limit. By the uncertainty principle (2.12), the eigenstate there should be a superposition of electric fluxes of various strength and locations as in the ordinary classical Coulombic electromagnetism shown in Table.1. So the physical state corresponding to the state considered in Eq.(2.20) is replaced by

$$\sum_{C_{12}} \Gamma(C_{12}) \prod_{\ell \in C_{12}} \hat{U}_\ell |0\rangle, \tag{2.21}$$

where the coefficient $\Gamma(C_{12})$ is the weight for the path C_{12} connecting the sites 1 and 2. For the lowest-energy state, $\Gamma(C_{12})$ is to be determined by the minimum-energy condition, and the energy stored in the two charges here should be proportional to $1/r$ as in the Coulomb potential energy (See Fig.2b).

The above qualitative consideration may indicate that there exists a phase boundary separating the strong and weak-coupling regions. Dynamics of the pure

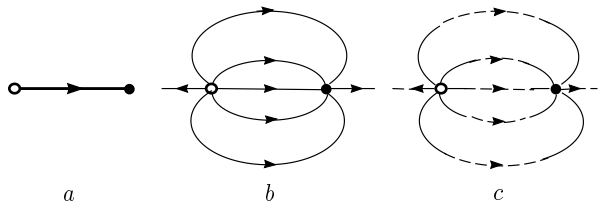

Fig. 2. Illustration of electric flux lines between two oppositely charged particles in the three phases. (a) confinement phase; (b) Coulomb phase; (c) Higgs phase. Dashed lines in (c) imply that the strength of fluxes are not conserved as Eq.(2.17) with $\langle \hat{\phi}_r^\dagger \hat{\phi}_r \rangle = \text{const} \neq 0$ shows.

gauge system H_g in (2.13) is quite nontrivial and careful investigation such as numerical study is required to obtain the phase diagram. At present, it is known that the 3D pure U(1) gauge system H_g has two phases; The phase at strong coupling region is called the confinement phase, and the phase at weak coupling region is called Coulomb phase. The phase transition is said to be weak first order[26]. These two phases are characterized by the behavior of the potential energy $V(r)$ for a pair of static charges of opposite signs and separated by a distance r; $\propto r$ or $\propto 1/r$. Also they are distinguished by the fluctuation of gauge field $\hat{\theta}_{ri}$, $\Delta\theta$, as $\Delta\theta \gg 1$ in the confinement phase and $\Delta\theta \ll 1$ in Coulomb phase. We note that, for the 2D spatial lattice in contrast, there are no phase transitions, and only the confinement phase exists[21].

Now let us include the matter part and consider the full Hamiltonian $\hat{H}$ of Eq.(2.13). By referring to Eq.(2.3), one may write $V(\hat{\phi}_r)$ as

$$V(\hat{\phi}_r) = \lambda(\hat{\phi}_r^\dagger \hat{\phi}_r - v)^2. \tag{2.22}$$

Let us recall that the GL theory with the gauge interaction being turned off by setting $g = 0$ and for sufficiently large and positive λ, the system exhibits a second-order phase transition by varying v. It is signaled by the order parameter $\phi = \langle\hat{\phi}_r\rangle$, (or more strictly defined as $|\phi|^2 \equiv \lim_{|r-r'|\to\infty}\langle\hat{\phi}_r^\dagger\hat{\phi}_{r'}\rangle$), and separates the ordered (condensed) phase $\langle\phi\rangle \neq 0$ and the disordered phase $\langle\phi\rangle = 0$. In the mean-field theory, the transition temperature T_c is determined as the vanishing point of v as $v \propto (T_c - T)$. However, the fluctuations of the phase degree of freedom φ_r of $\hat{\phi}_r = |\hat{\phi}_r|\exp(i\varphi_r)$, which are controlled by the hopping t-term of Eq.(2.13), play an essentially important role for realization of a condensation. In fact, these two phases may be characterized by the magnitude of fluctuation $\Delta\varphi$ of φ_r as $\Delta\varphi \ll 1$ (ordered phase) and $\Delta\varphi \gg 1$(disordered phase). To obtain the correct transition temperature T_c, more detailed study such as MC simulation is required as we discuss later.

For the full fledged gauge-matter system $\hat{H}$ of Eq.(2.13), one may naively consider four combinations such as ($\Delta\theta \ll 1$ or $\gg 1$) and ($\Delta\varphi \ll 1$ or $\gg 1$) for a possible phase. However, one may easily recognize that the combination $\Delta\varphi \ll 1$ and $\Delta\theta \gg 1$ is impossible. This is because $\hat{\varphi}_r$ appears in the hopping term with the combination $\nabla_i\hat{\varphi}_r - \hat{\theta}_{ri}$ and the condition $\Delta\theta \gg 1$ destroys the phase coherence $\nabla_i\hat{\varphi}_r \simeq 0$. In fact, the numerical study and the mean field theory predict the three phases listed in Table 1; (1) confinement phase $\Delta\theta \gg 1, \Delta\varphi \gg 1$, (2) Coulomb phase $\Delta\theta \ll 1, \Delta\varphi \gg 1$, (3) Higgs phase $\Delta\theta \ll 1, \Delta\varphi \ll 1$.

Let us see this point in some details because it helps us to understand the property of each phase appeared in an effective LGT of various condensed-matter systems.

(1) The confinement phase appears for the parameter region of small t [t is the hopping amplitude in Eq.(2.13)] and large g regardless of the values of λ and v. In a sense, this phase corresponds to the high-temperature (T) region and

there exist no long-range orders. The parameter region of the confinement phase is enlarged by decreasing a value of v. For pure U(1) gauge theory without matter field $\hat{\phi}_r$, a potential $V(r)$ for a pair of oppositely charged static sources separated with distance r behaves as $V(r) \propto r$ as explained.

(2) The Coulomb phase appears for small g and small t. Fluctuations of the gauge field is suppressed by the plaquette terms in Eq.(2.13) and the compactness of $\hat{\theta}_{ri}$ plays no role. The potential of a pair of two static charges is given by the Coulomb law, which is $V(r) \propto 1/r$ for 3D space.

(3) In the Higgs phase, a coherent condensation of the boson field $\hat{\phi}_r$ takes place. Then the hopping term in Eq.(2.13) gives the following term of $U_{x\mu}$,

$$t\hat{\phi}^\dagger_{r+i}\hat{U}^\dagger_{ri}\hat{\phi}_r + \text{H.c.} \to tv\ (\hat{U}^\dagger_{ri} + U_{ri}) + \cdots \simeq -tva^2g^2\hat{\theta}^2_{ri} + \cdots . \quad (2.23)$$

As a result, the gauge field acquires a mass $m_\theta = \sqrt{2tv}$ and a force mediated by the gauge field $\hat{\theta}_{ri}$ becomes short range like $\langle \hat{\theta}_{r+Ri,j}\hat{\theta}_{tj}\rangle = e^{-m_\theta R}$ (See Fig.2c). The Higgs phase is realized for large value of t and a finite v (in addition to small g). Superconducting (SC) phase is a kind of the Higgs phase in which the boson field $\hat{\phi}_r$ describes Cooper pairs, and the gauge field becomes short-ranged by the Meissner effect.

So far, we studied the compact LGT. In some literatures, so called noncompact LGT is considered[22]. The noncompact U(1) LGT is given by the following Hamiltonian for the gauge part,

$$\hat{H}'_{\rm g} = \frac{g^2}{2a}\sum_{r,i}(\hat{E}_{ri})^2 + \frac{1}{2g^2a}\sum_r\sum_{i<j}(\nabla_i\hat{\theta}_{rj} - \nabla_j\hat{\theta}_{ri})^2. \quad (2.24)$$

The eigenvalue of $\hat{\theta}_{ri}$ now runs in $(-\infty, \infty)$ and $\hat{H}'_{\rm g}$ loses the periodicity and describes a set of free photons. For small fluctuations $\Delta\theta \ll 1$, the compact pure gauge theory (2.13) reduces to above $\hat{H}'_{\rm g}$. However, for large fluctuations, these two models behave quite differently and they generally have different phase diagrams. In the noncompact gauge theories with the gauge part (2.24), the Coulomb and Higgs phases are realized but the confinement phase is impossible because of the suppression of large fluctuations. In other words, the large fluctuations of $\hat{\theta}_{ri}$ in the confinement phase are achieved by large-field configurations called topological excitations, the typical examples of which are instantons and monopoles. They are allowed only for a system with periodicity such as compact LGT. To describe a SC phase transition with the ordinary EM interactions, one should use the noncompact U(1) gauge theory. The gauge field $\hat{\theta}_{ri}$ there is nothing but the vector potential for the electro-magnetism, and the single-component boson field $\hat{\phi}_r$ corresponds to the s-wave Cooper-pair field as mentioned. Therefore, as we have explained above, the Higgs phase is nothing but the SC phase. In order to describe a multi-component SC state such as the p-wave SC, introduction of a multi-component boson field is necessary. This system will be discussed rather in detail in the subsequent sections.

2.3. *Partition function in the path-integral representation on the Euclidean lattice*

Let us consider the partition function Z for $\hat{H}$ of Eq.(2.13) at the temperature T,

$$Z = \mathrm{Tr}\hat{P}\exp(-\beta\hat{H}),\ \beta \equiv \frac{1}{k_B T},\ \hat{P} \equiv \prod_r \delta_{\hat{Q}_r,0}, \tag{2.25}$$

where Tr is over the space of all the values of $\hat{Q}_r$, and $\hat{P}$ is the projection operator to the physical states. As usual, we start by factorizing the Boltzmann factor into N factors but with care of $\hat{P}$ as

$$\hat{P}\exp(-\beta\hat{H}) = [\hat{P}\exp(-\Delta\beta\hat{H})]^N,\ \Delta\beta \equiv \frac{\beta}{N}, \tag{2.26}$$

where we used $\hat{P}^2 = \hat{P}, [\hat{P}, \hat{H}] = 0$, and then insert the complete set between every successive factors.

For $\hat{\phi}_r$, we use the following coherent states $|\phi\rangle$:

$$\hat{\phi}|\phi\rangle = \phi|\phi\rangle, |\phi\rangle = \exp(-\bar{\phi}\hat{\phi} + \hat{\phi}^\dagger\phi)|0\rangle,\ \hat{\phi}|0\rangle = 0,\ \langle\phi'|\phi\rangle = \exp(-\frac{\bar{\phi}'\phi'}{2} - \frac{\bar{\phi}\phi}{2} + \bar{\phi}'\phi'),$$
$$|\{\phi\}\rangle = \prod_r |\phi_r\rangle,\ \int d^2\phi = \prod_r \int \frac{d^2\phi_r}{\pi},\ \hat{1}_\phi = \int d^2\phi |\{\phi\}\rangle\langle\{\phi\}|, \tag{2.27}$$

where ϕ is a complex number and $\bar{\phi}$ is its complex conjugate (The bar denotes the complex-conjugate quantity).

The eigenstates and the completeness of gauge field for the entire lattice are written by using Eqs.(2.9) as

$$\hat{1}_\theta = \int d\theta |\{\theta\}\rangle\langle\{\theta\}|,\ \hat{1}_n = \sum_n |\{n\}\rangle\langle\{n\}|,\ |\{\theta\}\rangle = \prod_{r,i} |\theta_{ri}\rangle,\ |\{n\}\rangle = \prod_{r,i} |n_{ri}\rangle,$$
$$\int d\theta = \prod_{r,i}\int d\theta_{ri},\ \sum_n = \prod_{r,i}\sum_{n_{ri}\in\mathbf{Z}}. \tag{2.28}$$

(We abbreviate the symbol $\otimes$ of tensor product in $|\{\theta\}\rangle$ and $|\{n\}\rangle$.)

For example, the matrix element of $\hat{P}$ is calculated as

$$\delta_{\hat{Q}_r,0} = \int_0^{2\pi} \frac{d\theta_{r0}}{2\pi}\exp(i\theta_{r0}\hat{Q}_r),\ \langle\{\phi', n'\}|\hat{P}|\{\phi, n\}\rangle = \prod_r \int \frac{d\theta_{r0}}{2\pi} \prod_i \delta_{n'_{ri} n_{ri}} \cdot$$
$$\prod_r \exp(-\frac{1}{2}\bar{\phi}'_r\phi'_r - \frac{1}{2}\bar{\phi}_r\phi_r + \bar{\phi}'_r e^{-i\theta_{r0}}\phi_r)\exp(i\theta_{r0}\sum_i \nabla_i E_{ri}). \tag{2.29}$$

The Lagrange multiplier θ_{r0} will be interpreted as the imaginary-time component of gauge field. Then we obtain the following expression of Z for sufficiently large

N:

$$Z = \int [dU] \int [d\phi] \sum_{\{n\}} \exp(A_H),\ [dU] = \prod_{x,\mu} dU_{x\mu},\ [d\phi] = \prod_x d\phi_x, \sum_{\{n\}} = \prod_{x,i} \sum_{n_{xi}},$$

$$A_H = \Delta\beta \sum_x \Big[\frac{i}{\Delta\beta} \sum_i (E_{xi}\nabla_0\theta_{xi} + \theta_{x0}\nabla_i E_{xi}) - \frac{1}{\Delta\beta}\bar{\phi}_{x+0}(\phi_{x+0} - e^{-i\theta_{x0}}\phi_x) - V(\phi_x)$$

$$-t\sum_i |\phi_{x+i} - \bar{U}_{xi}\phi_x|^2 - \frac{g^2}{2a}\sum_i E_{xi}^2 + \frac{1}{2g^2 a}\sum_{i<j}(U_{xj}U_{x+j,i}\bar{U}_{x+i,j}\bar{U}_{xi} + \text{c.c.})\Big]. \quad (2.30)$$

where we assume that $V(\hat{\phi}_x)$ is normal ordered. In Eq.(2.30) we introduced the imaginary-time coordinate $x_0 (= 0, \cdots, N-1)$, the site index of 4D Euclidean lattice $x \equiv (x_0, r)$ with $r = (x_1, x_2, x_3)$, and its direction index/unit vector $\mu = 0, 1, 2, 3$. In path integral, every field $\phi_x, \theta_{x\mu}, n_{xi}$ is defined on each time slice x_0 together with the spatial site r. We note that $\phi_x, \theta_{x\mu}$ are periodic under $x_0 \to x_0 + N$. The 4-component U(1) gauge field $U_{x\mu} = \exp(i\theta_{x\mu})$ and its complex conjugate $\bar{U}_{x\mu}$ are sitting on the link $(x, x+\mu)$.

Next, we carry out the summation over n_{xi} to obtain[23]

$$Z = \int [dU][d\phi]\ \exp(A),\ A = \sum_x \Big[-\bar{\phi}_{x+0}(\phi_{x+0} - \bar{U}_{x0}\phi_x) - \Delta\beta V(\phi_x)$$

$$-t\Delta\beta\sum_i |\phi_{x+i} - \bar{U}_{xi}\phi_x|^2 + \frac{1}{2}\sum_{\mu<\nu} c_{2\mu\nu}(U_{x\nu}U_{x+\nu,\mu}\bar{U}_{x+\mu,\nu}\bar{U}_{x\mu} + \text{c.c.})\Big],$$

$$c_{2ij} = \frac{\Delta\beta}{g^2 a},\ c_{20i} = \frac{a}{g^2\Delta\beta},\ U_{x0} \equiv \exp(i\theta_{x0}). \quad (2.31)$$

Here we made the following replacement in $\sum_{n_{xi}}$ respecting the periodicity in θ:

$$\sum_n e^{-an^2+in\theta} \simeq \int_{-\infty}^{\infty} dn\ e^{-an^2+in\theta} = C\exp(-\frac{\theta^2}{4a}) \to C'\exp(\frac{1}{2a}\cos\theta). \quad (2.32)$$

The action A and the measure $[dU][d\phi]$ in Eq.(2.31 are invaraiant under the U(1) gauge transformation rotating the local internal coordinate of complex field at each site x on the 4-dimensional lattice,

$$U_{x\mu} \to \bar{V}_{x+\mu}U_{x\mu}V_x,\ V_x = e^{i\Lambda_x} \in \mathbf{U(1)},\ \phi_x \to V_x\phi_x, . \quad (2.33)$$

2.4. *Phase structure and Correlation functions*

Phase structure of various gauge-field models has been investigated by both analytic and numerical methods. In particular, for the gauge-Higgs model, which describes the SC phase transitions, interesting phase diagrams have been obtained. To this end, the numerical study by the Monte-Carlo (MC) simulations plays a very important role as they provide us reliable results including all nonperturbative effects. Here we present some known schematic phase diagrams restricting the system to the *relativistic Higgs coupling* and the frozen radial degrees of freedom of ϕ_x field,

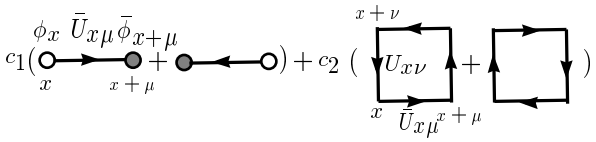

Fig. 3. Illustration of the action A of the compact LGT (2.34). Open (filled) circle denotes $\phi_x = \exp(i\varphi_x)(\bar{\phi}_x)$ and straight line with an arrow in the negative (positive) $\mu-$direction denotes $U_{x\mu} = \exp(i\theta_{x\mu})(\bar{U}_{x\mu})$

i.e., $\phi_x = \exp(i\varphi_x)$, but with spatial dimensions $d = 2$ and 3 (dimension of the corresponding Euclidean lattice $D = d + 1$ is 3 and 4). Explicitly, we consider the following partition function;

$$Z = \int [d\varphi][d\theta]_G \exp(A),\ A = c_1 \sum_{x,\mu} \cos(\varphi_{x+\mu} + \theta_{x\mu} - \varphi_x) + A_g^{(\prime)},$$

$$A_g = c_2 \sum_{x,\mu<\nu} \cos\theta_{x\mu\nu},\ A'_g = -\frac{c_2}{2} \sum_{x,\mu<\nu} \theta^2_{x\mu\nu},\ \theta_{x\mu\nu} \equiv \theta_{x\nu} + \theta_{x+\nu,\mu} - \theta_{x+\mu,\nu} - \theta_{x\mu}, \quad (2.34)$$

where $\mu = 0, \cdots, d$, and c_1 and c_2 are the parameters. A_g is for the compact LGT and A'_g is for the noncompact LGT. Each term of the action A is depicted in Fig.3. This model is sometimes called the Abelian Higgs model[11]. Note that the Higgs coupling (the c_1 term) along the imaginary time $\mu = 0$ direction has the same form as the spatial directions, i.e., every direction has couplings both in the positive and negative directions. This is in contrast to the nonrelativistic model (2.31) in which the coupling for $\mu = 0$ is only in the positive direction. In short, the coupling in the negative $\mu = 0$ direction describes the existence of antiparticles which are allowed in the relativistic theory but not in nonrelativistic theory[27].

Here we comment on the integration measure $[d\theta]_G$ and gauge fixing. The path integral (2.34) involves the same contributions from a set of configurations of $\{\varphi, \theta\}$ (so called gauge copies) that are connected with each other by gauge transformations. So one may reduce this redundancy by choosing only one representative from each set of gauge copies without changing physical contents. This procedure is called gauge fixing and achieved by inserting the gauge fixing function $G(\{\varphi, \theta\})$, which is not gauge invariant under Eq.(2.33), to the measure, $[d\varphi][d\theta] \to [d\varphi][d\theta]_G \equiv G(\{\varphi, \theta\})[d\varphi][d\theta]$. The difference between the gauge fixed case $[d\theta]_G$ and the nonfixed case $[d\theta]$ appears as a multiplicative factor in Z,

$$Z_{\text{nonfixed}} = C_{\text{gv}} Z_{\text{fixed}},\ C_{\text{gv}} = \prod_{x,\mu} \int d\Lambda_{x\mu}, \quad (2.35)$$

where the constant C_{gv} is called gauge volume. In the compact case, the region of $\theta_{x\mu}$ and $\Lambda_{x\mu}$ are both compact $[0, 2\pi)$. Therefore C_{gv} is finite and the gauge fixing is irrelevant (either choice of fixing gauge or not will do). In the noncompact case, the region of $\theta_{x\mu}$ and $\Lambda_{x\mu}$ is $(-\infty, \infty)$, so C_{gv} diverges. Thus, one must fix the

gauge in formal argument in the noncompact case, $[d\varphi][d\theta]_G$. We said "in formal argument" here because the choice $G(\{\varphi,\theta\}) = 1$ works even in the noncompact case as long as one calculate the average of gauge-invariant quantities, e.g., in the MC simulations. This is because the average does not suffer from the overall factor in Z. We shall present in Sect.4.1. another reason supporting this point, which is special in MC simulations.

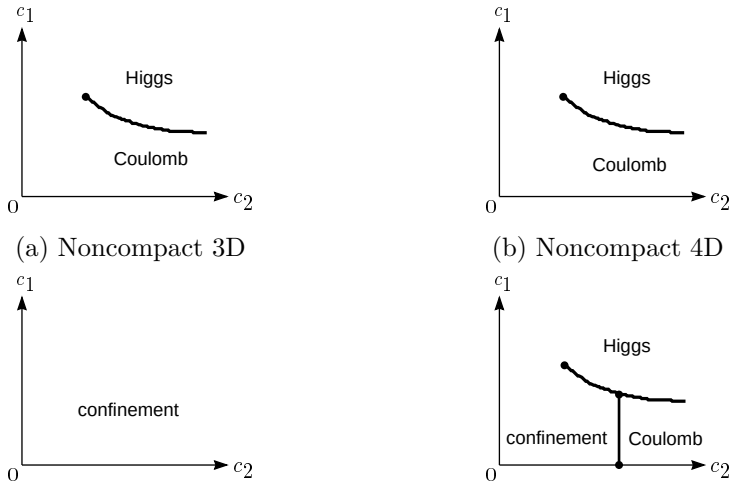

Fig. 4. Schematic phase diagrams in the $c_2 - c_1$plane of the 3D and 4D LGT with compact and noncompact action. All the Higgs-Coulomb transitions are of second order. The Higgs-confinement one in (d) is first order and the confinemnet-Coulomb one in (d) is weak first order. The partition function along the line $c_2 = 0$ is evaluated exactly by single link integral. It is an analytic function of c_1 and so no transitions exist along this line.

In Fig.4 we present the schematic phase diagrams in the $c_2 - c_1$ plane. The noncompact 3D and 4D models have the Coulomb phase and the Higgs phase. The compact 3D model has only the confinement phase. The compact 4D model has all the three phases. These points are understood as follows; (i) the Higgs phase may exist at large c_1 above the Coulomb phase in 3D and 4D, and above the confinement phase in 4D, (ii) the Coulomb phase may exist at sufficiently large c_2 in 4D case, (iii) the confinement phase exists in the compact case, but not in the noncompact phase.

We note that, as c_2 decreases, all the existing confinement-Higgs transition curves terminate at points with $c_2 > 0$. This can be understood by calculating Z for $c_2 = 0$ exactly. Because the integration over $\theta_{x\mu}$ there is factorized as

$$Z(c_1, c_2 = 0) = \prod_{x,\mu} \int d\theta'_{x\mu}\ e^{c_1 \cos\theta'_{x\mu}} = I_0(c_1)^{N_\ell},\ \theta'_{x\mu} \equiv \varphi_{x+\mu} + \theta_{x\mu} - \varphi_x, \quad (2.36)$$

where $I_0(c_1)$ is the modified Bessel function and $N_\ell(\equiv \sum_{x,\mu} 1)$ is the total number of links. $Z(c_1, c_2 = 0)$ is then an analytic function of c_1 and no phase transition can exists along the c_1 axis. This fact is known as complementarity and implies that the confinement phase and the Higgs phase are connected with each other without crossing a phase boundary.

Another limiting case $c_2 \to \infty$ may imply $\Delta\theta \to 0$. Therefore the resulting system becomes

$$Z(c_1, c_2 \to \infty) = \prod_{x,\mu} \int d\varphi'_x \exp[c_1 \sum_{x,\mu} \cos(\varphi'_{x+\mu} - \varphi'_x)], \tag{2.37}$$

by setting as $\theta_{x\mu} = \nabla_\mu \Lambda_x$ (pure gauge configuration) with $\varphi'_x \equiv \varphi_x + \Lambda_x$. This system is just the 3D and 4D XY spin models with the XY spin $(\cos\varphi_x, \sin\varphi_x)$, which are known to exhibit a second-order transition. This corresponds to the Higgs-Coulomb transition in Fig.4.

Let us discuss a general correlation function $\langle O(\{\theta\}, \{\varphi\})\rangle$ (the expectation value of the function $O(\{\theta\}, \{\varphi\})$) of the model (2.34) defined as

$$\langle O(\{\theta\}, \{\varphi\})\rangle = \frac{1}{Z} \int [d\varphi][d\theta] O(\{\theta\}, \{\varphi\}) \exp(A). \tag{2.38}$$

First, $\langle O(\{\theta\}, \{\varphi\})\rangle$ is known to satisfy the Elitzur theorem[24], which says

$$\langle O(\{\theta\}, \{\varphi\})\rangle = 0 \text{ if } O(\{\theta\}, \{\varphi\}) \text{ is not gauge invariant.} \tag{2.39}$$

Its proof is rather simple and given by making a change of variables in a form of gauge transformation and noting the measure $[d\theta][d\varphi]$ is invariant under it. A famous example of gauge-invariant correlation function is the Wilson loop defined on a closed loop C along successive links as

$$W(C) = \langle \prod_{\ell \in C} U_\ell \rangle. \tag{2.40}$$

It is used by Wilson as a nonlocal "order parameter" to distinguish a confinement phase and a deconfinement phase for pure gauge system (i.e., involving no dynamical charged particles). If $W(C)$ satisfies the "area law" as C becomes large, $W(C) \sim \exp(-aS(C))$ where $a > 0$ and $S(C)$ is the minimum area bound by C, the system is in the confinement phase. On the other hand, if it satisfies the perimeter law, $W(C) \sim \exp(-a'L(C))$ where $L(C)$ is the length of C, it is in the deconfinement phase. This interpretation comes from the fact that for the rectangular C of the horizontal size R and the vertical size T [The coordinate (x_0, x_1) of four corners in the 0-1 plane, e.g., are (0,0), (0,R), (T,0), (T,R)], $V(R)$ defined through $W(C) \sim \exp(-V(R)T)$ at sufficiently large T expresses the lowest potential energy stored by a pair of external charges separated by the distance R. The area law implies the confining potential $V(R) = aR$.

Second, one may estimate Z and the correlation functions of gauge-invariant objects by fixing the gauge because they are gauge invariant. Fixing implies to fix one degree of freedom per site x corresponding to Λ_x whatever one wants.

For example, the choice $\varphi_x = 0$ is called the unitary gauge, and another choice $\theta_{x0} = 0$ is called the temporal gauge. In the mean field theory for the compact LGT, one choose gauge variant quantities $\langle \exp(i\theta_{x\mu})\rangle$ and $\langle \exp(i\varphi_x)\rangle$ as a set of order parameters and predicts the phase structure involving the above mentioned three phases. They should be considered as a result after gauge fixing. If one wants to make it compatible with the Elitzur theorem, one simply need to superpose over the gauge copies of these order parameters as Drouffe suggested[25]. For $\langle \exp(i\theta_{x\mu})\rangle$, it implies

$$\prod_x \int_0^{2\pi} \frac{d\Lambda_x}{2\pi} \cdot \langle \exp(i\theta'_{x\mu})\rangle = 0,\ \theta'_{x\mu} = \theta_{x\mu} - \nabla_\mu \Lambda_x, \tag{2.41}$$

without changing the gauge-invariant results such as phase diagram, etc..

3. Ferromagnetic Superconductivity and its Lattice Gauge Model

In this section and Sect.4, we shall consider a theoretical model for the FMSC, which can be regarded as a kind of LGT. In some materials such as UGe_2, it has been observed that SC can coexist with a FM long-range order[29]. In UGe_2 and URhGe, a SC appears only within the FM state in the pressure-temperature (P-T) phase diagram, whereas, in UCoGe, the SC exists both in the FM and paramagnetic states. Soon after their discovery, phenomenological models of FMSC materials were proposed[30]. In those studies, the FMSC state is characterized as a spin-triplet p-wave state of electron pairs as suggested experimentally[31]. In this section, we introduce the GL theory of FMSC materials defined on the 3d spatial lattice (4D Euclidean lattice). As we see, the FM order naturally induces nontrivial vector potential (gauge field) and it competes with another order, the SC order, therefore a nonperturbative study is required in order to clarify the phase diagram etc.

3.1. *Ginzburg Landau theory of FMSC in the continuum space*

Before considering a lattice model of FMSC itself, let us start with the GL theory of FMSC in the 3d continuum space[30]. It was introduced phenomenologically for the case with strong spin-orbit coupling, although the origin of SC, etc. had not been clarified. Its free energy density $f_{\rm GL}$ contains a pair of basic 3d-vector fields, $\vec{\psi}(r)$ and $\vec{m}(r)$, which are to be regarded as c-numbers appearing in the path-integral expression for the partition function of the underlying quantum theory as in Eq.(2.31) [We discuss the partition function in detail later; see Eq.(3.16)].

The three-component complex field $\vec{\psi} = (\psi_1, \psi_2, \psi_3)^{\rm t}$ is the SC order parameter, describing the degrees of freedom of electrons participating in SC. More explicitly, $\vec{\psi}(r)$ describes Cooper-pairs of electrons with total spin $s = 1$ (triplet) and the relative angular momentum $\ell = 1$ (p-wave) (Note that only odd ℓ's are allowe for $s = 1$ by Pauli principle). The complex Cooper-pair field $\Phi_q(r)$ for a $s = 1$ and $\ell = 1$ state generally has $3 \times 3 = 9$ components ($q = 1, \cdots, 9$). The strong spin-orbit coupling forces the spin $\vec{S}(r)$ and the angular momentum $\vec{L}(r)$ made of $\Phi_q(r)$

parallel each other, and reduces their degrees of freedom down to 3. Such a Cooper pair is directly expressed in terms of the amplitudes defined as

$$\Delta_{\sigma\sigma'}(r) \equiv \int dr_0 \Gamma(r_0) \langle \hat{C}_\sigma(r + \frac{r_0}{2}) \hat{C}_{\sigma'}(r - \frac{r_0}{2}) \rangle. \tag{3.1}$$

$\hat{C}_\sigma(r)$ is the annihilation operator of electron at r and spin $\sigma =\uparrow, \downarrow$. $\Gamma(r_0)$ with r_0 being the relative coordinate of electrons is the weight reflecting the attractive interaction and the p-wave nature. Because we assign $\vec{\psi}(r)$ as a 3d vector, it is convenient to use the so called $\vec{d}$-vector, which transforms also as a vector in the 3d space;

$$\vec{\psi}(r) \propto \vec{d}(r) = \begin{pmatrix} d_x(r) \\ d_y(r) \\ d_z(r) \end{pmatrix} \equiv \begin{pmatrix} -\frac{1}{2}(\Delta_{\uparrow\uparrow}(r) - \Delta_{\downarrow\downarrow}(r)) \\ -\frac{i}{2}(\Delta_{\uparrow\uparrow}(r) + \Delta_{\downarrow\downarrow}(r)) \\ \Delta_{\uparrow\downarrow}(r) (= \Delta_{\downarrow\uparrow}(r)) \end{pmatrix}. \tag{3.2}$$

The real vector field $\vec{m}(r)$ is the FM order parameter, describing the degrees of freedom of electrons participating in the normal state. More explicitly, it describes their magnetization,

$$\vec{m}(r) = \langle \hat{C}'_\sigma(r) \Big(-i\delta_{\sigma\sigma'} \vec{r} \times \vec{\nabla} + \frac{1}{2} \vec{\sigma}_{\sigma\sigma'} \Big) \hat{C}'_{\sigma'}(r) \rangle, \tag{3.3}$$

where $\hat{C}'_\sigma(r)$ denotes the annihilation operator of electrons *not* participating in the SC state. Because there holds div $\vec{m}(r) = 0$ as in the usual magnetic field, $\vec{m}(r)$ is expressed by using the vector potential $\vec{A}(r)$ (gauge field) as

$$\vec{m}(r) = \mathrm{rot} \vec{A}(r). \tag{3.4}$$

Therefore, the fundamental fields may be $\vec{\psi}(r)$ and $\vec{A}(r)$,

The GL free energy density f_{GL} is then given by[?]

$$\begin{aligned} f_{\mathrm{GL}} &= f_\psi + f_m + f_{\mathrm{Z}}, \\ f_\psi &= K \sum_i (D_i \vec{\psi})^* \cdot (D_i \vec{\psi}) + \alpha (T - T^0_{\mathrm{SC}}) \vec{\psi}^* \cdot \vec{\psi} + \lambda (\vec{\psi}^* \cdot \vec{\psi})^2, \\ f_m &= K' \sum_i (\partial_i \vec{m})^2 + \alpha' (T - T^0_{\mathrm{FM}}) \vec{m}^2 + \lambda' (\vec{m}^2)^2, \\ f_{\mathrm{Z}} &= -J \vec{m} \cdot \vec{S}, \ D_i = \partial_i - 2ieA_i, \ \vec{S} = -i \vec{\psi}^* \times \vec{\psi}. \end{aligned} \tag{3.5}$$

$K^{(\prime)}, \alpha^{(\prime)}, \lambda^{(\prime)}$ are GL parameters; real positive parameters characterizing each material. $\vec{S}(r)$ is a real vector field describing the spin of Cooper pairs. For example, $S_3 = \frac{1}{2}(|\Delta_{\uparrow\uparrow}|^2 - |\Delta_{\downarrow\downarrow}|^2)$. f_{Z} with $J > 0$ is nothing but the Zeeman coupling of $\vec{S}$ and $\vec{m}$, which enhances the coexistence of the FM and SC orders as one easily expects. Although the existence of f_{Z} term is supported phenomenologically, its microscopic origin should be clarified by detailed study of the interactions of electrons (and nuclei) in each material.

f_{GL} is gauge invariant under the following U(1) gauge transformation,

$$\vec{\psi}(r) \to \vec{\psi}'(r) = e^{i\lambda(r)} \vec{\psi}(r), \ \vec{A}(r) \to \vec{A}'(r) = \vec{A}(r) + \frac{1}{2e} \vec{\nabla} \lambda(r). \tag{3.6}$$

So $\vec{m}(r)$ and $\vec{S}(r)$ are gauge invariant. This gauge invariance reflects the original U(1) gauge invariance of the EM interaction of electrons. For example, the K term with the covariant derivative D_i describes the interaction of SC Cooper pairs of charge $-2e$ with the vector potential $\vec{A}$ made of the normal electrons. Its microscopic origin should be traced back to the repulsive Coulombic interactions between electrons.

Before introducing the lattice GL theory, let us list up some main characteristics suggested by the continuum GL theory (3.5).

- In the mean-field approximation with ignoring the Zeeman coupling f_Z, $T^0_{\rm FM}$ and $T^0_{\rm SC}$ are critical temperatures of the FM and SC phase transitions, respectively.
- Existence of a finite magnetization, $\langle\vec{m}\rangle \neq 0$, means a nontrivial configuration of $A_i(r)$. This induces nontrivial spatial dependence of the Cooper pair $\vec{\psi}$ through the kinetic term $K(D_i\vec{\psi})^* \cdot (D_i\vec{\psi})$ in $f_{\rm GL}$, because this term favors $D_i\vec{\psi} \simeq 0$. A typical example of such configurations is a vortex configuration characterized by a nonvanishing vorticity $\vec{v}(r)$ of $\vec{\psi}$. The 3d vector $\vec{v}(r)$ of a complex field $\phi(r) = |\phi(r)| \exp(i\varphi(r))$ is defined generally as the winding number of its phase $\varphi(r)$. Explicitly, the component of $\vec{v}(r)$ along the direction of a normal vector $\vec{n}$ is defined by the circle integral over $\varphi(r)$,

$$\vec{n} \cdot \vec{v}(r') = \frac{1}{2\pi} \oint_{C_{\vec{n}}(r')} d\varphi(r) \ (\in \mathbf{Z}), \tag{3.7}$$

  where $C_{\vec{n}}(r')$ is a circle lying in the plane parpendicular to $\vec{n}$ with its center at r'. $\vec{n} \cdot \vec{v}(r)$ takes integers due to the single-valuedness of $\phi(r)$. In the later sections, we shall consider two vorticities $\vec{v}^{\pm}(r)$ corresponding to $\psi_1(r) \pm i\psi_2(r)$ respectively. Then the simple mean-field like estimation of the SC critical temperature has to be reexamined by more reliable analysis.
- The Zeeman coupling $f_{\rm Z}$ obviously enhances the coexisting phase of the FM and SC orders, since it favors a set of antiparallel $\vec{S}$ and $\vec{m}$ with large $|\vec{\psi}|$ and $|\vec{m}|$.
- In the FM phase, $\vec{A}$ produces a nonvanishing magnetic field $\vec{m}(r)$ inside the materials. Because the K term in f_ψ of Eq.(3.5) disfavors the coherent (spatially uniform) condensation of $\vec{\psi}$ ($\partial_i\vec{\psi} = 0$), due to rot $A \neq 0$ (favoring nontrivial ones such as vortices as explained above), the SC in a magnetic field is disfavored. In this sense, the system (3.5) is a kind of a frustrated system (the K term disfavors coexistence although the Zeeman term does).

Then a detailed study by using numerical methods is needed to obtain the correct phase diagram. To this end, we shall introduce a lattice version of the GL theory (3.5) that is suitable for the investigation by using MC simulations.

3.2. *GL theory on the lattice*

In this subsection we explain the lattice GL theory introduced in Ref.[32]. In constructing the theory, we start with the following two simplifications:

(1) We consider the "London" limit of the SC, i.e., we assume $\vec{\psi}^*(r) \cdot \vec{\psi}(r) =$ const. ignoring the fluctuations of the radial degrees of freedom $|\vec{\psi}(r)|$. This assumption is legitimate as the phase degrees of freedom $\vec{\psi}(r)$ themselves play an essentially important role in the SC transition (Recall the account of phase coherence for a Bose-Einstein condensate) [28].

(2) We assume that the third component $\psi_3(r) \propto \Delta_{\uparrow\downarrow}(r)$ is negligibly small compared to the remaining ones $\psi_{1,2}(r)$,

$$\psi_\pm \equiv \frac{1}{\sqrt{2}}(\psi_1 \pm i\psi_2),\ \psi_{\uparrow\uparrow} \equiv \psi_- \propto \Delta_{\uparrow\uparrow},\ \psi_{\downarrow\downarrow} \equiv -\psi_+ \propto \Delta_{\downarrow\downarrow}. \tag{3.8}$$

This simplification is consistent with the fact that the real materials exhibit FM orders of Ising-type with the $i = 3$-direction as the easy axis. In fact, $\vec{S} = -i\vec{\psi}^* \times \vec{\psi}$ is calculated with $\psi_{\uparrow\downarrow} \equiv \psi_3$ as

$$\vec{S} = (-\sqrt{2}\ \mathrm{Re}(\psi_{\uparrow\uparrow} + \psi_{\downarrow\downarrow})\psi^*_{\uparrow\downarrow}, \sqrt{2}\ \mathrm{Im}(\psi_{\uparrow\uparrow} - \psi_{\downarrow\downarrow})\psi^*_{\uparrow\downarrow}, |\psi_{\uparrow\uparrow}|^2 - |\psi_{\downarrow\downarrow}|^2)^{\mathrm{t}}. \tag{3.9}$$

So the Zeeman coupling f_{Z} requires large $\psi_{1,2}$ compared to ψ_3 to favor $\vec{m} \propto (0, 0, m)$.

In summary, we parametrize the Cooper-pair field in the London limit, $|\psi(r)|^2 = [\alpha/(2\lambda)](T^0_{\mathrm{SC}} - T)$, at low $T(< T^0_{\mathrm{SC}})$ with the third easy axis as

$$\begin{pmatrix} \psi_1(r) \\ \psi_2(r) \\ \psi_3(r) \end{pmatrix} = \sqrt{\frac{\alpha}{2\lambda}(T^0_{\mathrm{SC}} - T)} \times \begin{pmatrix} z_1(r) \\ z_2(r) \\ 0 \end{pmatrix},\ |z_1(r)|^2 + |z_2(r)|^2 = 1. \tag{3.10}$$

The "normalized" two-component complex field $z_a(r)$ $(a = 1, 2)$ satisfying the constraint (3.10) is called CP^1 variable (CP stands for complex projective group). In terms of the SC order-parameter field $z_a(r)$, the first K term of (3.5) is rewritten as $K\alpha(2\lambda)^{-1}(T^0_{\mathrm{SC}} - T)\sum_i \sum_a \overline{D_i z_a} \cdot D_i z_a$.

Now let us introduce the lattice GL theory of FMSC defined on the 3d cubic lattice. Its free energy density per site f_r is given by[32]

$$\begin{aligned} f_r = &-\frac{c_1}{2}\sum_{i=1}^{3}\sum_{a=1}^{2}\left(\bar{z}_{r+i,a}\bar{U}_{ri}z_{ra} + \mathrm{c.c.}\right) - c_2\vec{m}_r^2 - c_3\vec{m}_r \cdot \vec{S}_r + c_4(\vec{m}_r^2)^2 \\ &-c_5\sum_i \vec{m}_{r+i} \cdot \vec{m}_r,\ \sum_{a=1}^{2}\bar{z}_{ra}z_{ra} = 1,\ U_{ri} \equiv \exp(i\theta_{ri}). \end{aligned} \tag{3.11}$$

The five coefficients c_i $(i = 1 \sim 5)$ in (3.11) are real nonnegative parameters that are to distinguish various materials in various environments. z_{ra} is the CP^1 variable put on the site r and plays the role of SC order-parameter field. U_{ri} is the exponentiated

vector potential, θ_{ri}, put on the link $(r, r+i)$. $\vec{m}_r = (m_{r1}, m_{r2}, m_{r3})^{\rm t}$ is the magnetic field made out of θ_{ri} as

$$m_{ri} \equiv \sum_{j,k=1}^{3} \epsilon_{ijk} \nabla_j \theta_{rk}, \ \nabla_j \theta_{rk} \equiv \theta_{r+j,k} - \theta_{rk}. \tag{3.12}$$

$\vec{m}_r$ serves as the FM order-parameter field. Following Eq.(3.5), the spin $\vec{S}_r$ of the Cooper pair is defined as

$$\vec{S}_r = (0, 0, S_{r3}), \ \ S_{r3} \equiv -i(\bar{z}_{r1} z_{r2} - \bar{z}_{r2} z_{r1}) \ (\propto |\psi_{\uparrow\uparrow}|^2 - |\psi_{\downarrow\downarrow}|^2), \tag{3.13}$$

where we absorbed the normalization of $\vec{S}(r)$ into the coefficient c_3. $\vec{m}_r$, $\vec{S}_r$ and f_r are invariant under the following gauge transformation,

$$z_{ra} \to z'_{ra} = e^{i\lambda_r} z_{ra}, \ U_{ri} \to U'_{ri} = e^{-i\lambda_{r+i}} \ U_{ri} \ e^{i\lambda_r}. \tag{3.14}$$

Here we comment on the way of putting a 3d continuum vector field on the 3d lattice. It sounds natural that a vector field $\vec{B}(r)$ should be put on the link $(r, r+i)$ as B_{ri}. However, it is too naive. In fact, the gauge field $\vec{A}(r)$ has the nature of connection as explained and the connection between two points separated by finite distance such as nearest-neighbor pair of sites cannot be implemented by θ_{ri} itself but by its exponentiated form such as U_{ri}. This is the reason why one has $\bar{z}_{r+i,a} \bar{U}_{ri} z_{ra}$ term in Eq.(3.11). On the other hands, concerning to the SC order field $\vec{\psi}(r)$, its suitable lattice version depends on the coherence length ξ. If ξ is of the same order of lattice spacing a, its vector nature should be respected and the link field ψ_{ri} is adequate. If $\xi \gg a$, the detailed lattice structure is irrelevant and a simpler version ψ_{ra} $(a = 1, 2, 3)$ on the site (or its Ising counterpart z_{ra} $(a = 1, 2)$) will do. Eq.(3.11) corresponds to the latter case $\xi \gg a$ as some materials show.

Let us see the meaning of each term in f_r. The c_1-term describes a hopping of Cooper pairs from site r to $r+i$ (and from $r+i$ to r). As the Cooper pair has the electric charge $-2e$, it minimally couples with the vector potential θ_{ri} via U_{ri} as explained above. It is important to observe the relation between the hopping parameter c_1 and T. From the expression given in the paragraph below Eq. (3.5), we have

$$c_1 \sim K\alpha\lambda^{-1}(T^0_{\rm SC} - T)a. \tag{3.15}$$

At sufficiently large $\beta c_1 = c_1/T$ (we set $k_{\rm B} = 1$) that corresponds to low T's, the c_1-term stabilizes the combination of phases of $\bar{z}_{r+i,a} \bar{U}_{ri} z_{ra}$, and then, if U_{ri} is stabilized already by other mechanism, a *coherent condensation of the phase degrees of freedom of z_r is realized inducing the superconductivity.* The c_2 and c_4-terms are the quartic GL potential of $\vec{m}_r$, favoring a finite amount of *local* magnetization $\langle \vec{m}_r \rangle \neq 0$ (note that we take $c_2 > 0$). We should remark that these terms controls intrinsic magnetization, which is different from the fluctuating but external magnetic field. The c_5-term represents the NN coupling of the magnetization and corresponds to the K' term of Eq.(3.5). It enhances uniform configurations of $\vec{m}_r$, i.e., a FM long-range order signaled by a finite magnetization m, $m^2 \equiv \lim_{|r-r'|\to\infty} \langle \vec{m}_r \cdot \vec{m}_{r'} \rangle \neq 0$.

The c_3-term is the Zeeman coupling, which favors collinear configurations of $\vec{m}_r$ and $\vec{S}_r$, i.e., enhances the coexistence of FM and SC orders.

The partition function Z at T for the energy density f_r of Eq.(3.11) is given by the integral over a set of two fundamental fields z_{ra} and θ_{ri} as

$$\begin{aligned} Z &= \int [dz][d\theta] \exp(-\beta F),\ \beta = T^{-1},\ F = \sum_r f_r, \\ [dz] &= \prod_r d^2 z_{r1} d^2 z_{r2}\ \delta(|z_{r1}|^2 + |z_{r2}|^2 - 1), \\ [d\theta] &= G(\{\theta\}) \prod_{r,i} d\theta_{ri},\ \theta_{ri} \in (-\infty, \infty). \end{aligned} \tag{3.16}$$

where $G(\{\theta\})$ is a gauge fixing function[see the paragraph containing Eq.(2.35)].

We stress here that the free energy F and the integration variables in Eq.(3.16) have no dependence on the imaginary time x_0 in contrast with the expression (2.34). The ordinary GL theory explained in the literature also shares this properties. This implies that we ignore the x_0-dependent modes of would-be φ_x and $\theta_{x\mu}$ as $A(\{\varphi_x\}, \{\theta_{x\mu}\}) \to \beta F(\{\varphi_r\}, \{\theta_{ri}\})$. This is an approximation applicable for small β's, i.e., for high T's. This procedure allows us to make use of MC method that is based on the probabilistic process. In fact, the form (3.16) has a real function F and the Boltzmann factor $\exp(-\beta F)/Z$ is able to be interpreted as a probability. This is in contrast with the original action A corresponding to F; A is certainly a complex function as Eq.(2.34) giving rise to a complex probability. We come back to this point later.

The coefficients c_i $(i = 1, \cdots, 5)$ in f_r may have nontrivial T-dependence as Eqs.(3.5) and (3.15) suggest. However, in the present study we consider the response of the system by varying the "temperature" $T \equiv 1/\beta$ defined by β, an overall prefactor in Eq.(3.16), while keeping c_i fixed. This method corresponds to well-known studies such as the FM transition by means of the $O(3)$ nonlinear-σ model[33] and the lattice gauge-Higgs models discussed in Sec.2.1, and is sufficient to determine the critical temperature [See, e.g., Eq.(4.7)].

In the following section, we shall show the results obtained by MC numerical evaluation of Eq.(3.16). Physical quantities $\mathcal{O}(z, \theta)$ like the internal energy, specific heat, correlation functions, etc. are also calculated by the MC simulations as

$$\langle \mathcal{O}(z, \theta) \rangle = \frac{1}{Z} \int [dz][d\theta] \mathcal{O}(z, \theta) \exp(-\beta F). \tag{3.17}$$

From the obtained results, we shall clarify the phase diagram of the system and physical properties of each phase.

4. Results of Monte Carlo simulation

In the present section, we introduce and discuss the results of numerical calculations[32,34] for the lattice GL model (3.11), which include the phase diagram

and Meissner effect in the SC phase. Figs.5∼9 presented below are from Ref.[32] and Fig.10∼13 are from Ref.[34].

4.1. *Phase diagram and Meissner effect*

We first seek for a suitable boundary condition (BC) of θ_{ri} as the magnetization is expressed by θ_{ri} as Eq.(3.12). A familiar condition is the periodic boundary condition such as $\theta_{r+Li,j} = \theta_{rj}$ for the linear system size L. However, this condition necessarily gives rise to a vanishing net mean magnetization due to the lattice Storkes theorem. So we consider the 3d lattice of the size $(2+L+2)^2 \times L$ and take a "free BC" on z_r in the $i = 1, 2$ directions defined by

$$z_{r+i,a} - \bar{U}_{ri} z_{ra} = 0 \text{ for } r = \begin{cases} (0, r_2, r_3), & i = 1, \\ (L+2, r_2, r_3), & i = 1, \\ (r_1, 0, r_3), & i = 2, \\ (r_1, L+2, r_3), & i = 2, \end{cases} \tag{4.1}$$

whereas we impose the free boundary condition on θ_{ri}. It is easily shown that the BC (4.1) implies that the suppercurrent j^{SC}_{ri},

$$j^{\mathrm{SC}}_{ri} \propto \mathrm{Im}\,(\sum_a \bar{z}_{r+i,a} \bar{U}_{ri} z_{ra}), \tag{4.2}$$

satisfies $j^{\mathrm{SC}}_{r1(2)} = 0$ on the boundary surfaces in the $2(1) - 3$ planes. That is, the supercurrent does not leak out of the SC material. Another possible BC is the one that imposes vanishing Cooper-pair amplitude z_{ra}, but we expect, as usual, that the qualitative bulk properties of the results are not affected by the BC seriously. [The above BC (4.1) means that the magnetization is just like the Ising type and $\langle \vec{m}_x \rangle = (0, 0, m_3)$, which describes the real materials properly.]

In the simulation made in Refs.[32,34] we use the standard Metropolis algorithm[35] for the lattice size up to $L = 30$. The typical number of sweeps for a measurement is $(30000 \sim 50000) \times 10$ and the acceptance ratio is $40\% \sim 50\%$. The error is calculated as the standard deviation of 10 samples obtained by dividing one measurement run into 10 pieces. Concerning to the gauge-fixing term of Eq.(2.35), even for a noncompact gauge theory such as the present one, gauge fixing is not necessary in practical MC simulations. This is because, in addition to the reasons given at the end of paragraph of Eq.(2.35), the MC updates using random numbers almost never generate exactly gauge-equivalent configurations.

We calculate the internal energy U, the specific heat C of the central region R of the size L^3, the magnetization m_i, which are defined as follows,

$$U = \frac{1}{L^3}\langle F_L \rangle,\ C = \frac{1}{L^3}\langle (F_L - \langle F_L \rangle)^2 \rangle,\ F_L \equiv \sum_{r \in R} f_r,\ m_i \equiv \frac{1}{L^3}\langle | \sum_{r \in R} m_{ri} | \rangle, \tag{4.3}$$

and the normalized correlation functions,

$$G_m(r - r_0) = \frac{\langle \vec{m}_r \cdot \vec{m}_{r_0} \rangle}{\langle \vec{m}_{r_0} \cdot \vec{m}_{r_0} \rangle},\ G_S(r - r_0) = \frac{\langle S_{r3} S_{r_0,3} \rangle}{\langle S_{r_0,3} S_{r_0,3} \rangle}, \tag{4.4}$$

where r_0 is chosen on the boundary of R such as $(3, 2 + L/2, z)$. Singular behaviors of U and/or C indicate the existence of phase transitions, and the magnetization m_i and the correlation functions in Eqs.(4.4) clarify the physical meaning of the observed phase transitions. As the present system is a frustrated system as we explained above, G_m and G_S may exhibit some peculiar behavior in the FMSC state (the state in which FM and SC orders coexist).

To verify that the model (3.16) actually exhibits a FM phase transition as T is lowered, we put $c_1 = c_3 = 0$ and $(c_2, c_4, c_5) = (0.5, 4.0, 1.0)$, and measured C increasing β in the Boltzmann factor of Eq.(3.16). In Fig.5 we show C and m_i, which obviously indicate that a second-order phase transition to the FM state takes place at $\beta_{\rm FM} = 1/T_{\rm FM} \simeq 2.0$. We observed that other cases with various values of $c_{2,4,5}$ exhibit similar FM phase transitions.

Let us see the SC phase transition and how it coexists with the FM. We recall that the case of all $c_i = 0$ except for c_1 was studied in the previous paper Ref.[19]. There it was found that the phase transition from the confinement phase to the Higgs phase takes place at $c_1 \simeq 2.85$. This result suggests that the SC state exists at sufficiently large c_1 also in the present system with $c_{i(\neq 1)} \neq 0$.

To study this possibility, we use $(c_2, c_4, c_5) = (0.5, 4.0, 1.0)$ as in the FM sector above and $(c_1, c_3) = (0.2, 0.2)$. In Fig.6a, we show C vs β, which exhibits a large and sharp peak at $\beta \simeq 2.1$ and a small and broad one at $\beta \simeq 4.5$. To understand the physical meaning of the second broad peak, it is useful to measure "partial specific heat" C_i for each term F_i in the free energy (3.11) defined by

$$C_i = \frac{1}{L^3}\langle (F_i - \langle F_i \rangle)^2 \rangle, \;\; F_i = \sum_{r \in R} f_{ir}, \tag{4.5}$$

where f_{ir} is the c_i-term in f_r of Eq.(3.11).

Figs.6b,c show that the partial specific heat $C_{2,4,5}$ have a sharp peak at $\beta \simeq 2.1$. Thus the peak of total C there should indicate the FM phase transition. The analysis of Meissner effect (see the discussion below using Fig.8) supports this point. On the other hand, C_1 of the c_1-term has a relatively large and broad peak at $\beta \simeq 4.5$. C_3 also shows a broader peak there. Then we judge that the SC phase transition

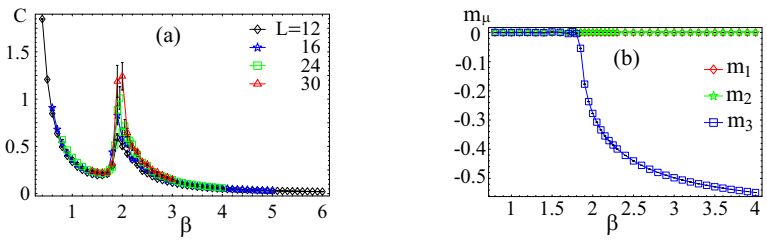

Fig. 5. (a) Specific heat for $(c_2, c_4, c_5) = (0.5, 4.0, 1.0)$ and $c_1 = c_3 = 0$. At $\beta \simeq 2.0$, C exhibits a sharp peak indicating a second-order FM phase transition. (b) Each component of magnetization m_μ vs β. For $T < T_{\rm FM}$, m_3 develops, whereas m_1 and m_2 are zero within the errors as expected.

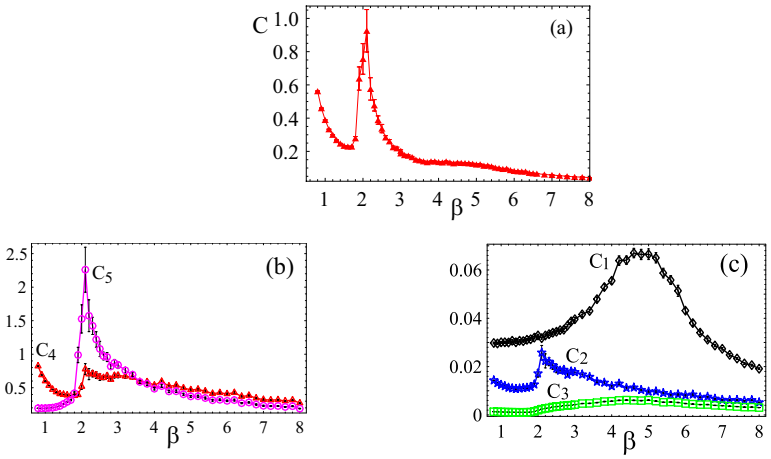

Fig. 6. (a) Specific heat vs β for $(c_1, c_3) = (0.2, 0.2)$ and $(c_2, c_4, c_5) = (0.5, 4.0, 1.0)$ ($L = 20$). There are a large peak at $\beta \simeq 2.1$ and a small one at $\beta \simeq 4.5$. (b,c) Partial specific heat C_i of Eq.(4.5) vs β. The small and broad peak at $\beta \simeq 4.5$ in C is related to fluctuations of c_1-term.

takes place at $\beta_{\rm SC} \simeq 4.5$. To support these conclusions, we show $G_m(r)$ and $G_S(r)$ in Fig.7. At $\beta = 2.5$, $G_m(r)$ exhibits a finite amount of the FM order, whereas $G_S(r)$ decreases very rapidly to vanish. This means that, as T is decreased, the FM transition takes place first and then the SC transition does. Therefore, for $\beta \geq \beta_{\rm SC} \simeq 4.5$, the FM and SC orders coexist. In this way, the partial specific heat may be used to judge the nature of each transition found by the peak of full specific heat C (We note $C \neq \sum_i C_i$ in general due to interference).

As we explained in the previous section, the bare transition temperature $T^0_{\rm SC}$ in Eq.(3.5) and the genuine transition temperature $T_{\rm SC}$ are different. Then it is interesting to clarify the relation between them. From Eq.(3.16), any physical quantity is a function of βc_i. In the numerical simulations, we fix the values of c_i and vary β as explained. Then the result $\beta_{\rm SC} \simeq 4.5$ means

$$\beta c_1|_{T=T_{\rm SC}} = 4.5 \times 0.2. \tag{4.6}$$

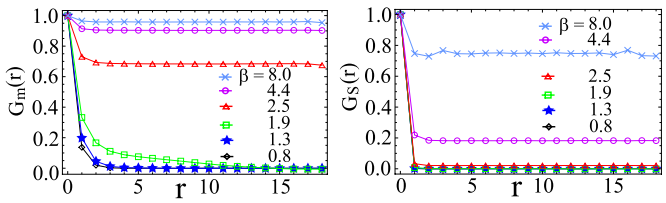

Fig. 7. Correlation functions $G_m(r)$ and $G_S(r)$ at various T's for $L = 20$. c_i's are the same as in Fig.6.

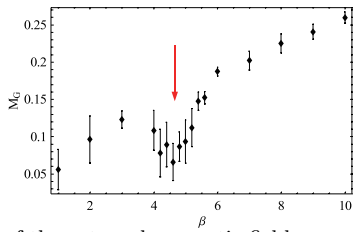

Fig. 8. Gauge-boson mass $M_{\rm G}$ of the external magnetic field propagating in x-y plane vs β for the same c_i as in Fig.6 and $c_2{}' = 3.0$ ($L = 16$). At the SC phase transition point $\beta_{\rm SC} \simeq 4.5$ (indicated by an arrow) determined by the peak of C, $M_{\rm G}$ starts to increase from small values.

By using Eq.(3.15), this gives the following relation;

$$\frac{1}{T_{\rm SC}} \frac{K\alpha (T^0_{\rm SC} - T_{\rm SC})a}{\lambda} = 0.90 \ \rightarrow T_{\rm SC} = \Big(1 + \frac{0.90\ \lambda}{K\alpha\ a}\Big)^{-1} T^0_{\rm SC}. \tag{4.7}$$

Eq.(4.7) shows that the transition temperature is lowered by the fluctuations of the phase degrees of freedom of Cooper pairs. We expect that a relevant contribution to lowering the SC transition temperature comes from vortices that are generated spontaneously in the FMSC as we shall show in Sec.4.2.

After having confirmed that the genuine critical temperature can be calculated by the critical value of β with fixed c_i, we use the word temperature in the rest of the paper just as the one defined by $T \equiv 1/\beta$ while c_i are T-independent parameters.

One of the most important phenomena of the SC is the appearance of a finite mass of the electromagnetic field, i.e., the Meissner effect. In theoretical study of the SC that includes the effect of fluctuations of the Cooper-pair wave function as in the present one, a finite mass of the photon is the genuine order parameter of the SC. To study it, we follow the following steps[19]; (i) introduce a vector potential $\theta^{\rm ex}_{ri}$ for an external magnetic field, (ii) couple it to Cooper pairs by replacing $U_{ri} \rightarrow U_{ri} \exp(i\theta^{\rm ex}_{ri})$ in the c_1 term of f_x and add its magnetic term $f^{\rm ex}_r = +c_2{}'(\vec{m}^{\rm ex}_r)^2$ ($c_2' > 0$) to f_r with $\vec{m}^{\rm ex}_r$ defined in the same way as (3.12) by using $\theta^{\rm ex}_{ri}$, (iii) let $\theta^{\rm ex}_{ri}$ fluctuate together with z_{xa} and θ_{ri} and measure an effective mass $M_{\rm G}$ of $\theta^{\rm ex}_{ri}$ via the decay of correlation functions of $\vec{m}^{\rm ex}_r$. The result of $\vec{m}^{\rm ex}_r$ *propagating in the 1-2 plane* is shown in Fig.8. It is obvious that the mass $M_{\rm G}$ starts to develop at the SC phase transition point, and we conclude that Meissner effect takes place in the SC state.

4.2. *Vortices in FMSC state*

In this section, we study the FMSC state observed in the previous section in detail. In particular, we are interested in whether there exist vortices and their density if any. There are two kinds of vortices as the present SC state contains two gaps described by $\psi^+_r \propto z^+_r$ and $\psi^-_r \propto z^-_r$, where $z^\pm_r$ are defined as

$$z^\pm_r \equiv \frac{1}{\sqrt{2}}(z_{r1} \pm i z_{r2}) \equiv \sqrt{\rho^\pm_x} \exp(i\gamma^\pm_r). \tag{4.8}$$

Corresponding to the above Cooper pair fields, one may define the following two kinds of gauge-invariant vortex densities V_r^+ and V_r^- in the 1-2 plane;

$$V_r^{\pm} \equiv \frac{1}{2\pi}[\mathrm{mod}(\gamma_{r+1}^{\pm} - \gamma_r^{\pm} - \theta_{r1}) + \mathrm{mod}(\gamma_{r+1+2}^{\pm} - \gamma_{r+1}^{\pm} - \theta_{r+1,2}) \\ -\mathrm{mod}(\gamma_{r+1+2}^{\pm} - \gamma_{r+2}^{\pm} - \theta_{r+2,1}) - \mathrm{mod}(\gamma_{r+2}^{\pm} - \gamma_r^{\pm} - \theta_{r2})], \quad (4.9)$$

where $\mathrm{mod}(x) \equiv \mathrm{mod}(x, 2\pi)$. In short, $V_r^{\pm}$ describes vortices of electron pairs with the amplitude $z_r^{\pm}$.

To study the behaviors of vortices step by step, we first consider the case of constant magnetization (magnetic field), i.e., we set θ_{ri} by hand so that

$$m_{r1} = m_{r2} = 0, \ m_{r3} = f = \text{constant}, \quad (4.10)$$

freezing their fluctuations. As the above numerical studies show that a typical magnitude of the magnetization $\langle m_{r3} \rangle = 0.8 \cdots$, we put $f = \frac{\pi}{4}$. In this case, the SC phase transition takes place at $\beta = 4.8$. Snapshots of vortices are shown in Fig.9. It is obvious that at lower-T, i.e., $\beta = 7.0$, densities of vortices are low compared to the higher-T ($\beta = 3.0$) case but they are still nonvanishing. This result obviously comes from the existence of the finite magnetization, i.e., the internal magnetic field.

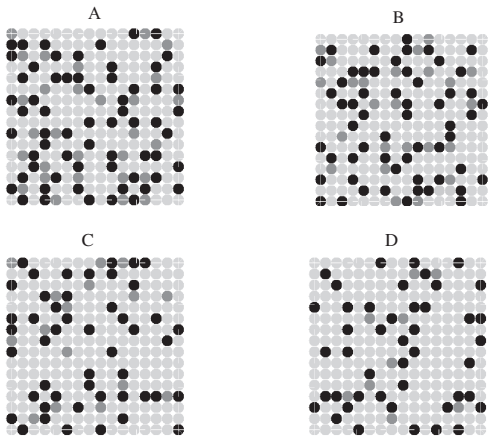

Fig. 9. Snapshots of vortex densities $V_r^{\pm}$ at $(c_1, c_2, c_3, c_4, c_5) = (0.2, 0.5, 0.2, 4.0, 1.0)$ for a *fixed magnetization* $\vec{m}_r = (0, 0, \pi/4)$ ($L = 16$) from Ref.[32]. Black dots; $V_r^{\pm} = 0.875$, Dark gray dots; -1.125, Light gray dots; -0.125. (A)V_r^+ at $\beta = 3.0$, (B)V_r^- at $\beta = 3.0$, (C)V_r^+ at $\beta = 7.0$, (D)V_r^- at $\beta = 7.0$. The average magnitude $\langle |V_{r\pm}| \rangle$ is (A) 0.387, (B) 0.380, (C) 0.331 and (D) 0.335. The points $V_r^{\pm} = -0.125 = -m_3/(2\pi)$ reflect $\vec{m}$ itself, and corresponds to the state without genuine vortices.

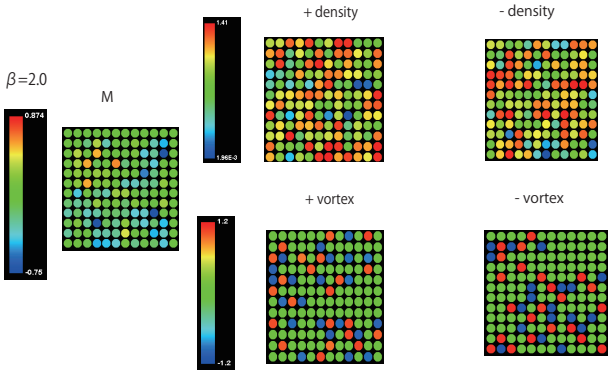

Fig. 10. Snapshot at $\beta = 2.0$ with *dynamically fluctuating* $\vec{m}_r$. The values of c_i are $(c_1, c_2, c_3, c_4, c_5) = (0.2, 0.5, 0.2, 4.0, 1.0)$.

It is interesting to study behavior of vortices and the magnetization in the FMSC state rather in detail. We now allow for fluctuations of θ_{ri}. In this state, the magnetization m_{r3} fluctuates around its mean value. As we showed in the previous section, the FM and SC phase transitions take place at $\beta_{\rm FM} \simeq 2.1$ and $\beta_{\rm SC} \simeq 4.5$, respectively. We are interested in the β-dependence of various quantities such as the magnetic field $\langle m_{r3} \rangle$, the vortex densities $V_r^{\pm}$, and the Cooper-pair densities $\langle \rho_r^{\pm} \rangle$.

In Figs. $10 \sim 13$ we show these quantities as snapshots at $\beta = 2.0, 3.0, 4.0, 5.2$ for the set of parameters $(c_1, c_2, c_3, c_4, c_5) = (0.2, 0.5, 0.2, 4.0, 1.0)$. At $\beta = 2.0$ (Fig.10), the local magnetization m_{r3} fluctuates rather strongly, and also the density of Cooper pairs ρ_r^+ and ρ_r^- are almost equal. Densities of vortices $V_r^{\pm}$ are also fairly large. At $\beta = 3.0$(Fig.11), m_{r3} tends to have a positive value. This corresponds to the fact that the system has the FM long-range order. At $\beta = 4.0$(Fig.12), ρ_r^+

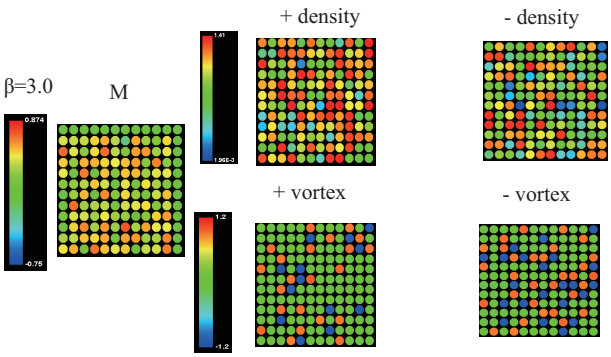

Fig. 11. Snapshot at $\beta = 3.0$ with *dynamically fluctuating* $\vec{m}_r$. The values of c_i are the same as in Fig.10.

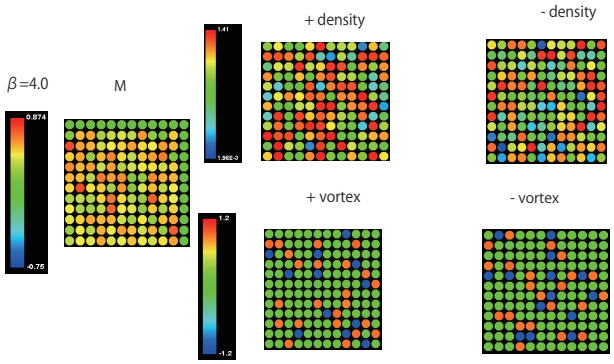

Fig. 12. Snapshot at $\beta = 4.0$ with *dynamically fluctuating* $\vec{m}_r$. The values of c_i are the same as in Fig.10.

is getting larger compared to ρ_r^-. Similarly, V_r^- is sightly larger than V_r^+. These results reflect the Zeeman coupling. At $\beta = 5.2$(Fig.13), vortex-antivortex pairs are formed, and V_r^- is larger than $V+_r$. As in the case of the constant magnetic field, the densities of vortices are nonvanishing even in the SC phase.

5. Conclusion

In this paper, we present a brief review of LGT with Higgs matter field, and then apply it to the GL lattice model of FMSC. The detailed MC simulations of the model reveal the global structure such as the phase diagram and the physical characteristics of each phase in an explicit manner. The concepts and knowledges of LGT considerably help us to build an appropriate lattice model as well as to interpret the results of MC simulations. We want to add this example to the rather

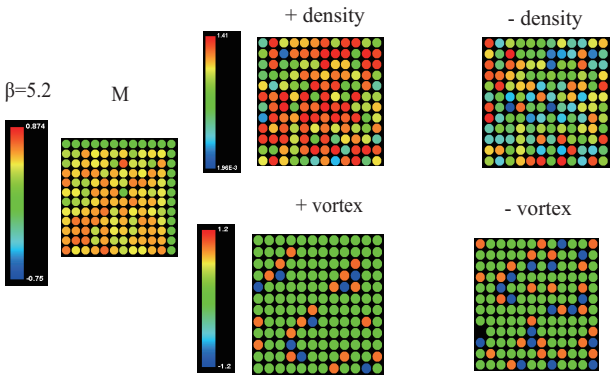

Fig. 13. Snapshot at $\beta = 5.2$ with *dynamically fluctuating* $\vec{m}_r$. The values of c_i are the same as in Fig.10.

long list of studies that have utilized the following common three-step method: (i) Establishing a lattice gauge model of the phenomenon of one's interest, (ii) Performing MC simulations of the model, (iii) Intepreting the MC results according to LGT. Here we list up a couple of tips to remove obstacles in carrying out this program.

- MC simulations become more effective with less variables. To avoid unnecessary inflation of degrees of freedom, one should identify what are the relevant variables. Neglecting the radial degrees of freedom of the Higgs field ϕ_r is an example[28].
- MC simulations require positive measure to make use of a probabilistic (Markoff) process. Fermionic systems in their original forms suffer from the well known negative-sign problem, which generates negative probabilities. By restricting the region of parameters of the model, it could be possible to avoid this problem. For example, the critical region around a continuous phase transition, the order-parameters are small and the GL expansion may assure us a positive provability[6].
- Another example to avoid nonpositive provability is the case of bosonic system at finite temperatures. The path integral of bosonic variables usually contain the imaginary kinetic term like $i \int d\tau \bar{\phi}(d\phi/d\tau)$ in the action, where $\tau \in (0, \beta = 1/(k_B T))$ is the imaginary time. By focusing in the high-temperature region, the τ-dependent modes of $\phi(\tau)$ may be ignored and so is this kinetic term. This is the case of FMSC studied in Sect. 3 and 4, and some of the cases studied in Ref.[6,7]. This procedure has an extra merit that the dimension of the effective lattice system is reduce to d-dimensions instead of $D = d + 1$ dimensions due to the absence of the x_0-direction.

Nowadays, it is well known that a quite wide variety of systems of cold atoms put on an optical lattice may serve as a quantum simulator of certain definite quantum model with almost arbitrary values of interaction parameters. Such a simulator is to clarify the *dynamical* (time-dependent) properties of the quantum model. Therefore, the importance of theoretical analysis of such models become increased as a guide for experiments. For example, information on the global phase structure of a quantum model is quite useful to perform experiments in an effective manner, although the former is confined to the static (time-independent) properties in thermal equilibrium. We expect that the above path (i-iii) with the successive tips may be useful for this purpose, in particular to simulate the model including compact or noncompact gauge fields. We hope as many readers as possible make use of this practical but powerful tool to strengthen and expand their researches.

Acknowledgments

We thank Mr. T. Noguchi, our coauthor of Ref.[34], for his help and discussions. We also thank Dr. K. Kasamatsu for reading the manuscript and presenting comments and suggestions. This work was supported by JSPS KAKENHI Grant-numbers 23540301, 26400246, 26400412.

References

1. See, e.g. a review; P. A. Lee, N. Nagaosa, and X-G Wen, Rev. Mod. Phys. **78**, 17 (2006).
2. P. A. Lee, Science 321, **1306** (2008).
3. M. P. A. Fisher, P. B. Weichman, G. Grinstein, and D. S. Fisher, Phys. Rev. **B 40**, 546 (1989); D. Jaksch, C. Bruder, J. I. Cirac, C. W. Cardiner, and P. Zoller, Phys. Rev. Lett. **81**, 3108 (1998).
4. M. W. Long and X. Zotos, Phys. Rev. **B 45**, 9932 (1992); M. Boninsegni, Phys. Rev. Lett. **87**, 087201 (2001); Phys. Rev. **B 65**, 134403 (2002); L.-M. Duan, E. Demler, and M. D. Lukin, Phys. Rev. Lett. **91**, 090402 (2003); E. Altman,W. Hofstetter, E. Demler, andM. D. Lukin, New J. Phys. **5**, 113 (2003). For the relation between the Bose Hubbard model and the bosonic $t-J$ model, see Appendix A of the last reference of Ref.[7].
5. See, e.g., M. Lewenstein, A. Sanpera, and V. Ahufinger, "*Ultracold Atoms in Optical Lattices: Simulating Quantum Many-body Systems*", (Oxford University Press, 2012).
6. For the $t-J$ model of electrons, see G. Baskaran and P. W. Anderson, Phys. Rev. **B 37**, 580 (1988); A. Nakamura and T. Matsui, Phys. Rev. **B 37**, 7940 (1988); I. Ichinose and T. Matsui, Phys. Rev. **B 45**, 9776 (1992); Nucl. Phys. **B 394**, 281 (1993); Phys. Rev. **B 51**, 11860 (1995); P. A. Lee and N. Nagaosa, Phys. Rev. **B 46**, 5621 (1992); N. Nagaosa and P. A. Lee, Phys. Rev. Lett. **64**, 2450 (1990); Phys. Rev. **B 43**, 1233 (1991). I. Ichinose, T. Matsui and M. Onoda, Phys. Rev. **B 64**, 104516 (2001).
7. K. Aoki, K. Sakakibara, I. Ichinose, and T. Matsui, Phys. Rev. **B 80**, 144510 (2009). Y. Nakano, T. Ishima, N. Kobayashi, K. Sakakibara, I. Ichinose, and T. Matsui, Phys. Rev. **B 83**, 235116 (2011).
8. K. G. Wilson, Phys. Rev. **D 10**, 2445 (1974).
9. For earlier reviews and books of LGT, see, e.g., J. B. Kogut, Rev. Mod. Phys. **51**, 659 (1979); M. Creutz, "*Quarks, gluons and lattices*", (Cambridge University Press 1985); I. Montvay and G. Münster, "*Quantum Fields on a Lattice*", (Cambridge University Press 1997).
10. G. 't Hooft, Nucl. Phys. **B 138**,1 (1978); M. E. Peskin, Ann. Phys. **113**, 122 (1978).
11. M. B. Einhorn and R. Savit, Phys. Rev. **D 17**, 2583 (1978).
12. G. Kotliar and A . Ruckenstein, Phys. Rev. Lett. **57**, 2790 (1987); Z. Zou and P. W. Anderson, Phys. Rev. **B 37**, 627 (1988).
13. P. W. Anderson, Phys. Rev. Lett. **64**, 1839 (1990).
14. See, e.g., J. K. Jain, "*Composite fermions*", (Cambridge University Press, 2007) and references cited therein.
15. For composite boson formalism, see M. P. A. Fisher and D. H. Lee, Phys. Rev. **B 39**, 2756 (1989); S. C. Zhang, Int. J. Mod. Phys. **B 6**, 25 (1992). For composite fermion, formalism, see J. Jain, Phys. Rev. Lett. **63**, 199 (1989), Phys. Rev. **B 40**, 8079 (1989); **41**, 7653 (1990).
16. J. Kogut and L. Susskind, Phys. Rev. **D 11**, 3376 (1974).
17. For inclusion of relativistic fermions, see Refs.[8,9,16] For relativistic bosons, see Sect.2.4 and Ref.[11]. For nonrelativistic fermions, see I. Ichinose and T. Matsui, Phys.

Rev. **B 45**, 9776 (1992).
18. K. G. Wilson and J. Kogut, Phys. Rep. **12**, 75 (1974).
19. S. Takashima, I. Ichinose and T. Matsui, Phys. Rev. **B 72**, 075112 (2005).
20. In the relativistic theory, the charge-conjugate pair of ϕ-particle (antiparticle) having the charge $-g$ should appear on an equal footing.
21. A. M. Polyakov, Phys. Lett. **B 59**, 82 (1975).
22. Sometimes the noncompact model is studied just for the purpose of comparison with the compact model. In general, one must ask for every system and situation under consideration which model (compact vs. noncompact) is more suitable.
23. In some literatures, the term $|\phi_{x+\mu} - U_{x\mu}\phi_x|^2$ appears instead of $|\phi_{x+\mu} - \bar{U}_{x\mu}\phi_x|^2$. They are related by $\phi_x \leftrightarrow \bar{\phi}_x$ or $U_{x\mu} \leftrightarrow \bar{U}_{x\mu}$ and equivalent each other.
24. S. Elitzur, Phys. Rev. **D 12**, 3978 (1975).
25. J. M. Drouffe, Nucl. Phys. **B 170**, 211 (1980).
26. See, e.g., E. Sa'nchez-Velasco, Phys. Rev. **E 54**, 5819 (1996), and references cited therein.
27. In the relativistic theory, Eq.(2.34) is obtained by starting with a set of annihilation operator, $\hat{a}_r$ of particle and $\hat{b}_r$ of antiparticle. Then, the charge operator is written as $q(\hat{a}_r^\dagger \hat{a}_r - \hat{b}_r^\dagger \hat{b}_r)$. One writes the path-integral expression of Z by using the canonical pair $(\hat{\phi}_r^\pm, \hat{\pi}_r^\pm)$ with $\hat{a}_r = \hat{\phi}_r^+ + i\hat{\pi}_r^+$, $\hat{b}_r = \hat{\phi}_r^- + i\hat{\pi}_r^-$. Then by integrating over $\pi_r^\pm \in \mathbf{C}$ one arrives at Eq.(2.34) with $\phi_r = \phi_r^+ + i\phi_r^- \in \mathbf{C}$. This ϕ_r is a canonical field in contrast with the coherent-state field ϕ_r in Eq.(2.31) although the same symbol ϕ_r is used.
28. Of course, the fluctuations of radial component $|\phi_x|$ may give rise to certain effects. For example, in the abelian Higgs model, fluctuations of $|\phi_x|$ may change the second-order SC transition to a first-order one if the coefficient λ of the $|\phi_x|^4$ coupling [See Eq.(2.22)] becomes sufficiently small. See, e.g., K. Jansen, J. Jersák, C. B. Lang, T. Neuhaus, G. Vones, Nucl. Phys. **B 265**, 129 (1986).
29. For UGe_2, see S. S. Saxena *et al.*, Nature (London) **406**, 587 (2000); A. Huxley *et al.*, Phys. Rev. **B 63**, 144519 (2001); N. Tateiwa *et al.*, J. Phys. Condens. Matter **13**, L17 (2001). For URhGe, see D. Aoki *et al.*, Nature (London) **413**, 613 (2001). For UCoGe, see N. T. Huy *et al.*, Phys. Rev. Lett. **99**, 067006 (2007); E. Slooten et al. Phys. Rev. Lett. **103**, 097003 (2009).
30. K. Machida and T. Ohmi, Phys. Rev. Lett. **86**, 850 (2001); M. B. Walker and K. V. Samokhin, Phys. Rev. Lett. **88**, 207001 (2002).
31. F. Hardy and A. D. Huxley, Phys. Rev. Lett. **94**, 247006 (2005); Harada *et al.*, Phys. Rev. **B 75**, 140502 (2007).
32. A. Shimizu, H. Ozawa, I. Ichinose, and T. Matsui, Phys. Rev. **B 85**, 144524 (2012). Here, we adopted the alternative notation explained in Ref.[23].
33. See, e.g., J. Cardy, "*Scaling and Renormalization in Statistical Physics*", (Cambridge University Press, 1996).
34. T. Noguchi, I. Ichinose and T. Matsui in preparation.
35. N. Metropolis, A. W. Rosenbluth, M. N. Rosenbluth, A. M. Teller, and E. Teller, J. Chem. Phys. **21**, 1087 (1953); J. M. Thijssen, "*Computational Physics*", (Cambridge University Press, 1999).